UILU-ENG-73-2014

CIVIL ENGINEERING STUDIES
STRUCTURAL RESEARCH SERIES NO. 397

STRESS-STRAIN RELATIONSHIPS OF REINFORCING BARS SUBJECTED TO LARGE STRAIN REVERSALS

By
A. E. AKTAN
B. I. KARLSSON
M. A. SOZEN

A Report on a Research
Project Sponsored by
THE NATIONAL SCIENCE FOUNDATION
Research Grant GI 29934

UNIVERSITY OF ILLINOIS
at URBANA-CHAMPAIGN
URBANA, ILLINOIS
JUNE 1973

STRESS-STRAIN RELATIONSHIPS OF REINFORCING BARS SUBJECTED TO LARGE STRAIN REVERSALS

by

A. E. Aktan
B. I. Karlsson
M. A. Sozen

A Report on a Research Project Sponsored by
THE NATIONAL SCIENCE FOUNDATION
Research Grant GI 29934

UNIVERSITY OF ILLINOIS
URBANA, ILLINOIS
June, 1973

TABLE OF CONTENTS

LIST OF FIGURES

Chapter 1

INTRODUCTION

1.1 General

Quantitative information on the stress-strain relation of reinforcing steel under strain reversals is essential for the analysis of reinforced concrete elements subjected to earthquake effects. In spite of recent investigations on this subject (2, 4), there is a lack of information on the properties of reinforcing steel subjected to large strain reversals. References 2 and 4 provide data on steel coupon tests where a maximum strain increment of 0.01 was realized between reversals. Moreover the coupons were mainly cycled in tension, the compressive strains attained during the tests were less than 0.005.

The purpose of this report is to document the tests on the stress-strain behavior of reinforcing steel under large strain reversals, carried out at the Structural Research Laboratory of the University of Illinois in Urbana. Steel coupons, machined from #6 and #9 nominal size structural steel bars were subjected to strain programs representing the steel history of a reinforced concrete column subjected to earthquake excitation. Compressive strains of 0.06 and strain differences of 0.09 between loading reversals were reached in these tests. Two studies on the analytical representation of the measured stress-strain relationships are presented following the test results.

1.2 Scope

This report contains the results of nine steel coupon tests and two analytical models to represent the measured stress-strain relationships.

Six of the nine coupon specimens were machined from the same #9 standard size deformed bar. Strain increments of 0.09 between load reversals and a maximum compressive strain of 0.06 were obtained during the testing of these coupons.

The remaining three coupon specimens were machined from three different #6 standard size deformed bars, taken from the same batch of bars delivered from the mill. Strain increments of 0.03 and a maximum compressive strain of 0.015 was reached during the testing of these specimens.

The major variables in the testing program were the entire previous strain history and the virgin properties of the material.

The objects of the study were specifically as follows:

(a) To investigate the stress-strain behavior of structural grade reinforcing steel under load reversals resulting in large strain increments representing the actual steel strain histories in prototype reinforced concrete elements under earthquake loading.

(b) To develop an analytical model to represent the measured stress-strain relationships.

1.3 Acknowledgement

The writers wish to express their appreciation to Dr. H. Aoyama and Mr. J. K. Wight for their help and contributions during this study.

Thanks are also due to Dr. V. J. McDonald and Mr. J. N. Sterner for their help during the tests and data processing.

The IBM 360/75 computer system of the Department of Computer Science was used for the data processing and analyses.

The work was supported by the National Science Foundation Grant 29934.

Chapter 2

TESTS

2.1 Test Coupons

The dimensions of the machined #9 and #6 bar coupons are given in Fig. 1. The dimensions of the coupons were arrived through a preliminary test program. Coupon sizes were varied until the proportions which accomodated a 0.5 in. extensometer and enabled the largest strain increment between load reversals without buckling was determined.

2.2 Loading Systems

The #9 bar coupons were tested with a 600-kip capacity servo-controlled hydraulic testing machine. The #6 bar coupons were tested in a smaller frame equipped with a servo-controlled hydraulic ram of 20-kip capacity. Both machines can be operated through a control module that is part of a closed servo loop, commanding either the stroke or the load. The stroke sensitivity of the machines was 1×10^{-4} inches. The load sensitivities were 0.1% of the load at full capacity.

The specimens were tested with "aline-a-matic" grips*. These grips with spherical end blocks were aligned at the start of a test by applying a small tensile load to the coupon. They were then locked in this configuration, minimizing the possibility of eccentric loading during the compression cycles of the tests.

---

*Trademark of MTS Systems Corporation, Minneapolis, Minnesota.

2.3 Instrumentation and Test Procedure

The instrumentation of the test specimens varied in the tests. The first four #9 bar coupons were equipped with four strain gages and a 0.5 in. electronic extensometer as shown in Figure 1. The strain readings from the strain gages and the extensometer during the large compression cycles of the first four tests indicated that the test setup was free of objectionable bending effects. A comparison of the extensometer versus average strain of the strain gages during the last compression cycle of test coupon 1 is given in Fig. 2. The remaining two #9 bar coupons and the three #6 bar coupons were equipped with two 0.5 in. electronic extensometers at opposite faces. This enabled a check of the uniaxial strain condition throughout the tests. The maximum strain difference between the extensometer recordings in the tests was less than 10%.

The test schedules were programmed in terms of strain histories to represent the steel strain records obtained during the reversed-loading tests of reinforced concrete columns at the Structural Research Laboratory of the University of Illinois (1). After the strain history for a coupon was determined this history was applied by operating the testing machine in stroke control. Connecting an extensometer on the coupon to the plotter of the control module, the stroke was applied to produce the designated strain history, controlling through the plot. The stroke was applied with a uniform speed during a loading cycle. The only loading discontinuity occurred during the switch of the stroke direction between loading cycles.

The strain readings of the strain gages and extensometers were recorded by a PI 8 channel tape recorder on magnetic tape, at a speed of 3.75 ips and in the form of continuous voltage signals. Prior to each test, calibration voltage signals were recorded on the tape to later digitize the analog signals.

A schematic representation of the test setup is given in Fig. 3.

2.4 Data Processing and Test Results

The analog continuous voltage signals of the electronic strain measuring equipment was digitized to an average of 10000 record points for each channel, each strain gage, extensometer and load cell corresponding to a channel. The digitized data was then calibrated to convert into load and strain quantities and transferred to a magnetic tape for processing in the IBM 360/75 system. During the analysis of digitized data, the number of data points for each channel was reduced to an average of 1000 points for each test. This reduction decreased the processing and analysis costs without sacrificing the necessary continuity of the measurements.

The results of the nine coupon tests are presented in Fig. 4-12.

Chapter 3

ANALYTICAL REPRESENTATION OF THE MEASURED STRESS-STRAIN RELATIONSHIPS

Two different models were used to represent the observed response characteristics of the bars tested under cyclic loading. They are described in the following two sections.

3.1 The Ramberg-Osgood Model

A Ramberg-Osgood function (3) having the following form was used to describe the stress-strain relationship for each half-cycle between two stress-reversals as shown in Fig. 13.

$$\frac{\varepsilon - \varepsilon_i}{\varepsilon_o} = \frac{\sigma - \sigma_i}{\sigma_o} + \left(\frac{\sigma - \sigma_i}{\sigma_o}\right)^{\alpha} \qquad (1)$$

where ε and σ denote the strain and the stress, and ε_i and σ_i are the initial values of the strain and stress at the beginning of the half cycle. The terms ε_o, σ_o and α are the three parameters of the Ramberg-Osgood function.

An iterative process of least squares curve fitting technique was applied to determine the three parameters for each half cycle of the test data in the following manner: two of the parameters were assumed for the half cycle. The third parameter was calculated to make the square of the error a minimum for all the data points of the half cycle. The two assumed parameters were then changed by a small increment. The procedure

was repeated for a reasonable number of increments and the analyzed variable resulting in the minimum square of the error was selected. The complete procedure was carried out for all three variables separately.

The results of this analysis indicated that the ratio σ_o/ε_o can be taken as the modulus of elasticity of steel, 29,000,000 psi. The number of parameters were thus reduced to two.

The iterative least-square analysis was repeated for σ_o fixing the ratio of σ_o/ε_o by 29,000,000 psi. A plot of the results of this analysis versus the sum of the maximum stresses obtained in tension and compression during the test prior to the half cycle under consideration is shown in Fig. 14. This plot indicated linear correlations between the sum of the maximum stresses and σ_o, depending on the sign of the stress at the initial point for the half cycle under consideration.

With this information an investigation of the test data and certain trial values for α resulted in the following rule to obtain this parameter: A stress of $\pm$ 110,000 psi is obtained for 9% strain increment for the half cycle, the sign of the stress being the same as the sign of the stress axis at the end of the half cycle.

The Ramberg-Osgood model, obtained by the results of the #9 bar coupon tests was then generalized in terms of the yield stress of the coupons. The rules to determine the model are summarized in the following:

1. $\sigma = E\,\varepsilon$ for $\varepsilon < \varepsilon_y$
2. $\sigma = \sigma_y$ for $\varepsilon_y < \varepsilon < 4.2447\,\varepsilon_y$

3. $\frac{\varepsilon}{\varepsilon_o} = \frac{\sigma}{\sigma_o} + (\frac{\sigma}{\sigma_o})^{\alpha}$ for $4.2447\ \varepsilon_y < \varepsilon$

before the first reversal, where

$\sigma_o = .7\ \sigma_y$; $\varepsilon_o = \sigma_o/E$; $\alpha = 4.3$

4. $\frac{\varepsilon - \varepsilon_1}{\varepsilon_o} = \frac{\sigma - \sigma_1}{\sigma_o} + (\frac{\sigma - \sigma_1}{\sigma_o})^{\alpha}$

for subsequent half cycles, where

σ_o/ε_o = 29,000,000 psi,

$\sigma_o = 47628 + .51723\ (\sigma_{max} - \sigma_{min})$

for half cycles starting from compression,

$\sigma_o = 46410 + .47989\ (\sigma_{max} - \sigma_{min})$

for half cycles starting from tension,

σ = 110,000 psi for $\varepsilon = .09 - \varepsilon_1$,

σ = -110,000 psi for $\varepsilon = -.09 - \varepsilon_1$,

where

σ = stress (psi),

ε = strain,

σ_y = yield stress of the bar (psi),

ε_y = yield strain of the bar,

σ_{max} = maximum tensile stress reached prior to the half cycle under consideration (psi),

σ_{min} = maximum compressive stress reached prior to the half cycle under consideration (psi).

The comparisons of the "Ramberg-Osgood" model with the nine coupon tests are presented in Fig. 15-23.

3.2 The Linear Model

Common linear models like the elasto-plastic strain hardening model that represents the stress-strain relation for steel assume that the initial boundary curves into tension or compression regions are the envelopes for stress in reversed loadings. The actual behavior is different in the sense that there is no fixed envelope or strain hardening slope. These two quantities depend on the plastic strain attained before the loading reversal occurs. This characteristic is demonstrated in Fig. 24. A simple linear representation of the stress-strain behavior is suggested in the following.

The initial stress-strain relation is elasto-plastic with a strain hardening slope of 1,125,000 psi, up to a stress of $\pm$ 110,000 psi in tension or compression.

At any reversal, if any plastic strain is obtained for the half cycle before the reversal occurs, the boundary line after the reversal shifts further into tension or compression by the stress increment corresponding to the plastic strain increment obtained before the reversal. The slope of this new boundary line is less than the previous boundary line and is given by $k_o \frac{\pm 110{,}000 - \sigma_i}{\pm 110{,}000 - \sigma_n}$, where k_o is the slope of the previous boundary line, σ_n is the stress measured from the strain axis to the intersection of the unloading line and the previous boundary line and σ_i is larger than σ_n by the shift in the boundary line.

These rules are demonstrated in Fig. 25. If a plastic strain increment is not obtained before the reversal, the previous boundary line does not change.

The nine coupon tests are compared with this model in Fig. 26-34.

Chapter 4

CONCLUSIONS

On the basis of the test results and the analyses carried out, the following conclusions can be made:

1. The stress-strain relation of reinforcing steel is dependent upon the entire previous loading history and the virgin properties of the material.
2. The energy absorption characteristics of reinforcing steel is conservatively expressed by the linear, elasto-plastic models.
3. An accurate Ramberg-Osgood representation of the stress-strain relation is possible. However the accuracy of this representation depends upon the definition of the three Ramberg-Osgood parameters which are related to the virgin properties of the material. The Ramberg-Osgood model proved not to be as successful with virgin properties different from the ones it was based on. Therefore the use of such a complicated model may not be warranted unless detailed test data are available for a particular bar.
4. A linear representation of the stress-strain response is satisfactory for applications where detailed information on the stress-strain characteristics of the bar is not available.

LIST OF REFERENCES

1. Karlsson, B. I., H. Aoyama and M. A. Sozen, "Spirally Reinforced Concrete Columns Subjected to Loading Reversals Simulating Earthquake Effects," paper submitted for presentation at the Fifth World Conference on Earthquake Engineering, Rome, Italy, 1973.

2. Kent, D. C., "Inelastic Behavior of Reinforced Concrete Members with Cyclic Loading, " thesis presented to the University of Canterbury, at Christchurch, New Zealand, in partial fulfillment of the requirements for the degree of Doctor of Philosophy, 1969.

3. Ramberg, W. and W. R. Osgood, "Description of Stress-Strain Curves by Three Parameters," National Advisory Committee on Aeronautics, TN 902, 1943.

4. Singh, A., K. H. Gerstle and L. G. Tulin, "The Behavior of Reinforcing Steel Under Reversed Loadings," Journal ASTM, Materials Research and Standards, Vol. 5, No. 1, January, 1965.

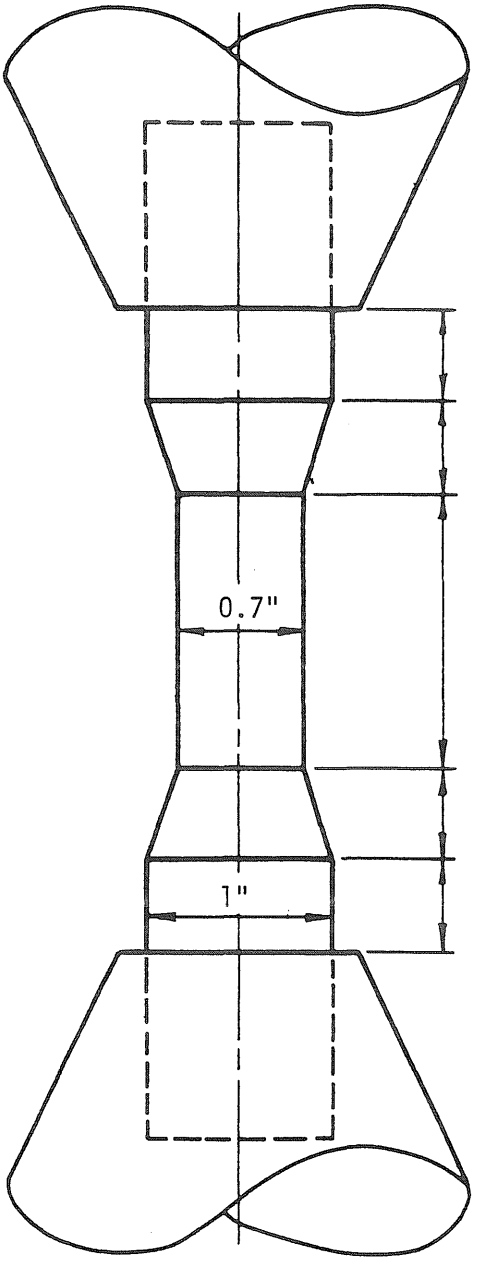

1.a #9 Bar Coupon

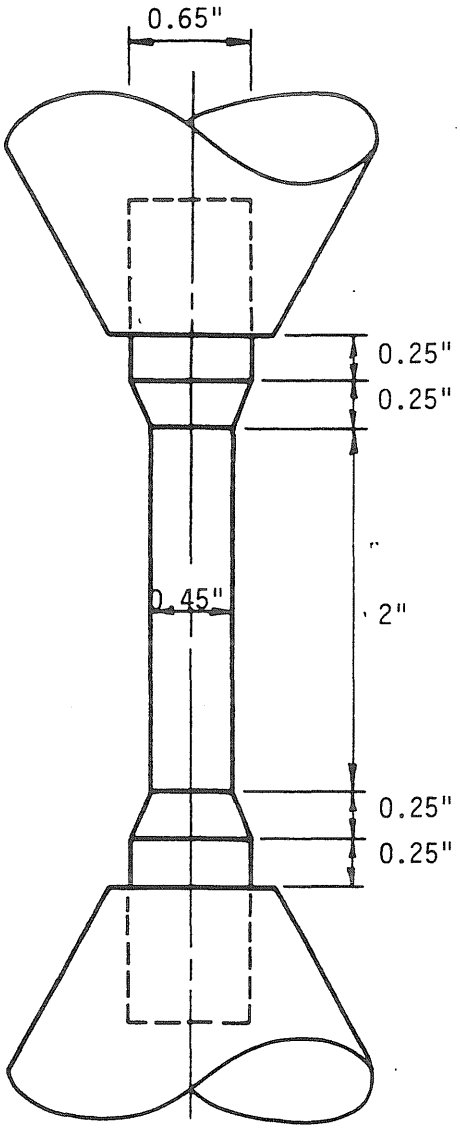

1.b #6 Bar Coupon

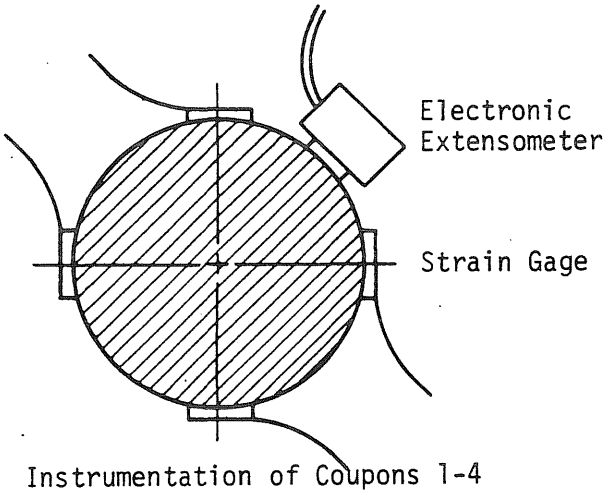

1.c Instrumentation of Coupons 1-4

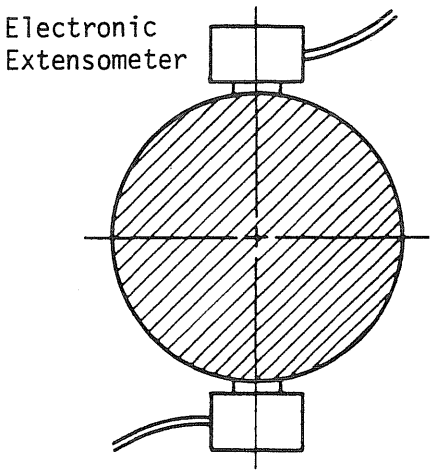

1.d Instrumentation of Coupons 5-9

Fig. 1 Dimensions and Instrumentation of Test Coupons

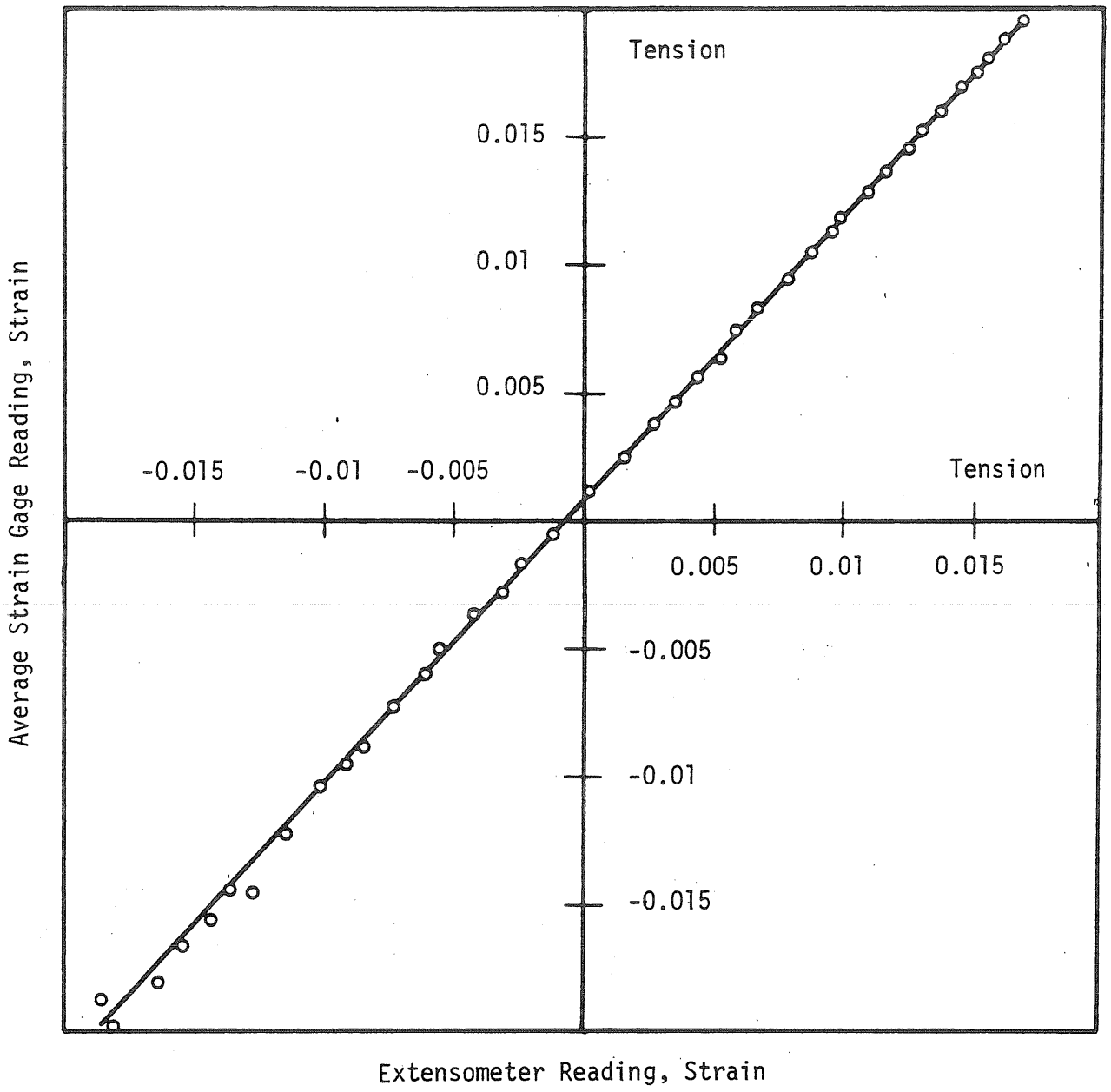

Fig. 2 Comparison of Extensometer against Strain Gage, Last Compression Cycle, Test 1

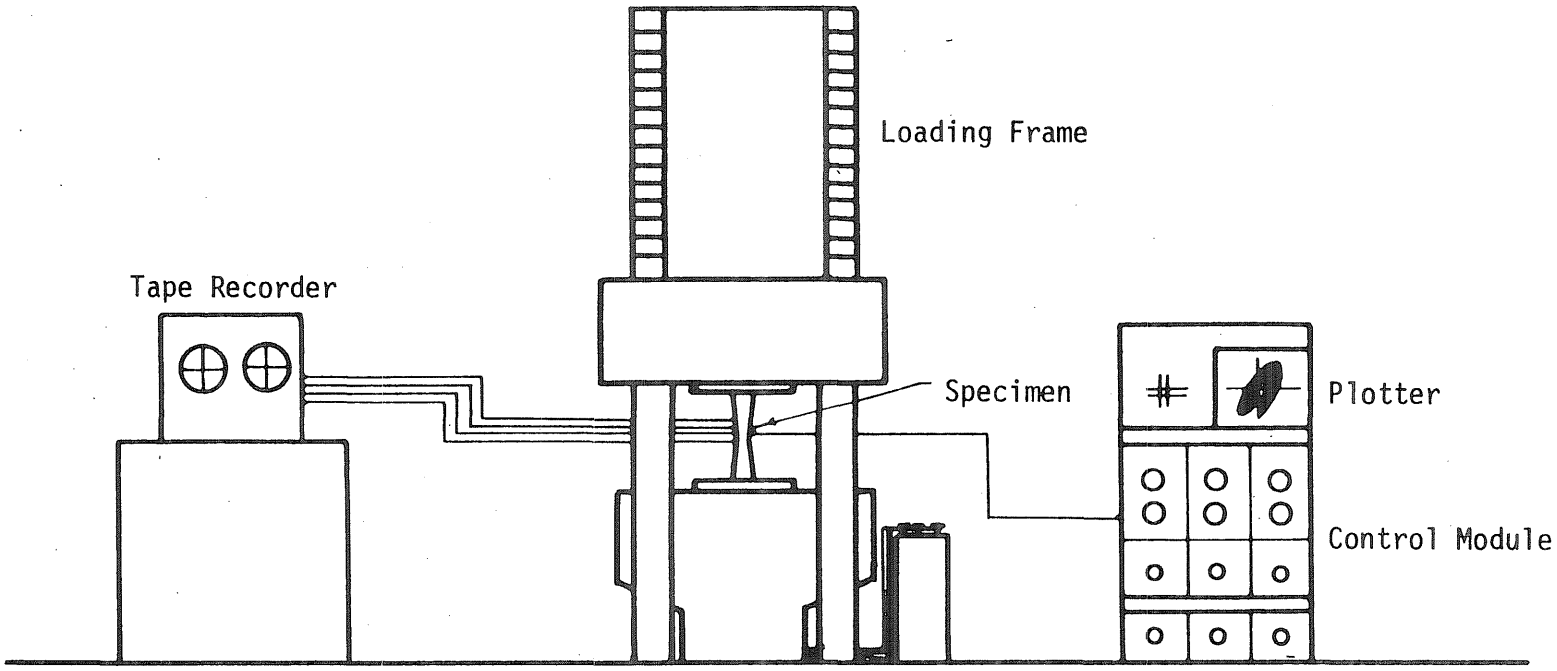

Fig. 3 Schematic Representation of the Test Setup

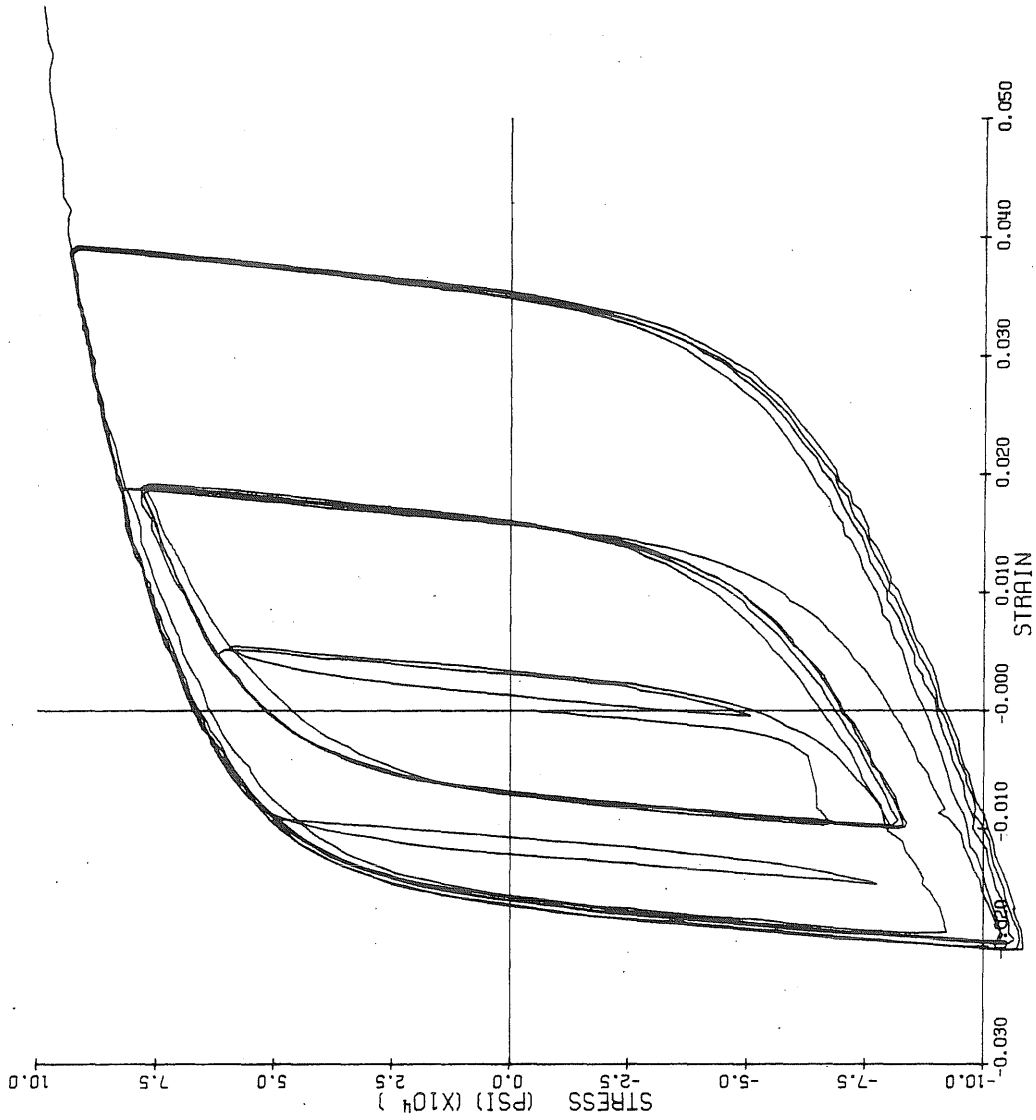

Fig. 4 Test 1, #9 Bar Coupon

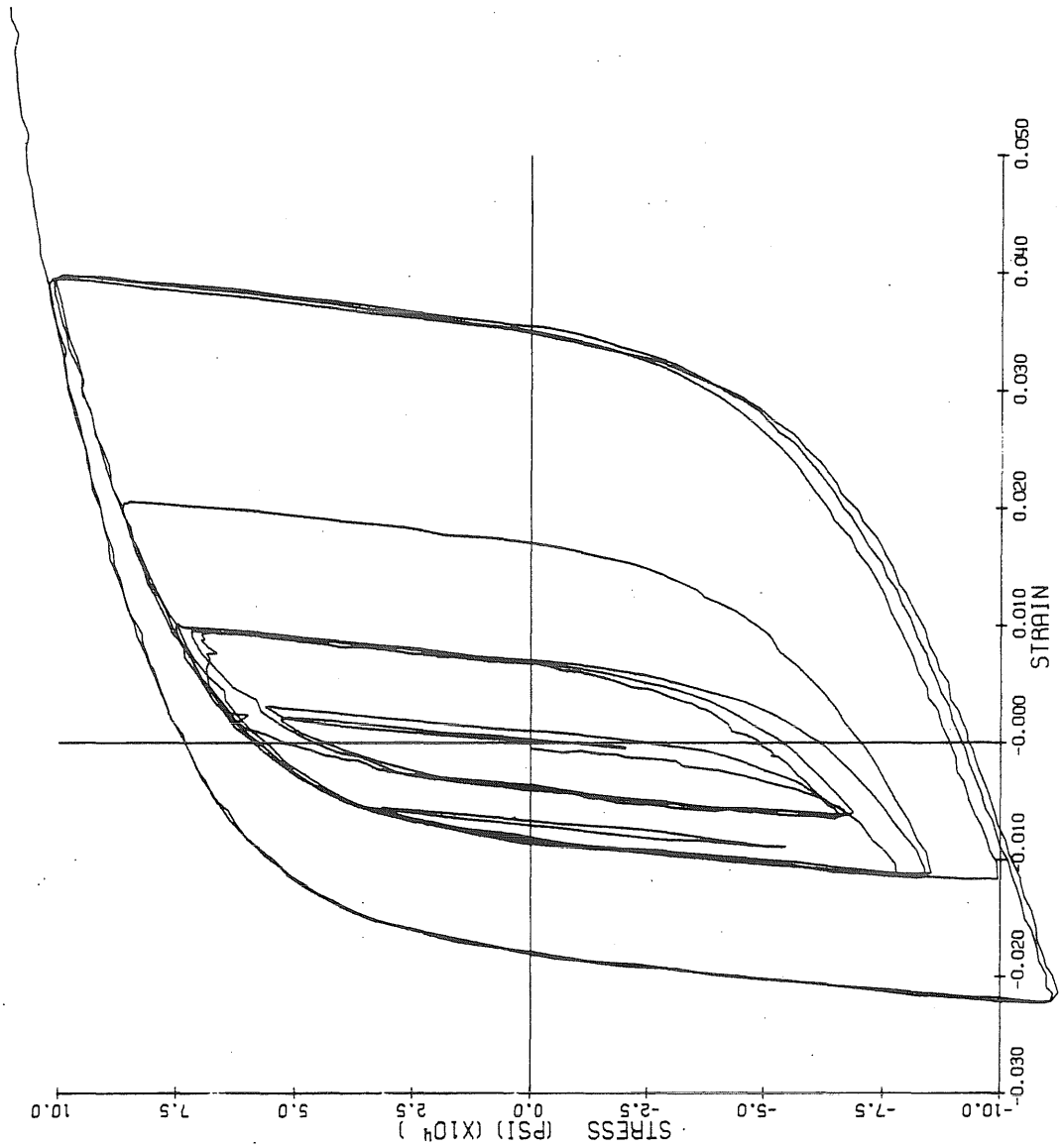

Fig. 5 Test 2, #9 Bar Coupon

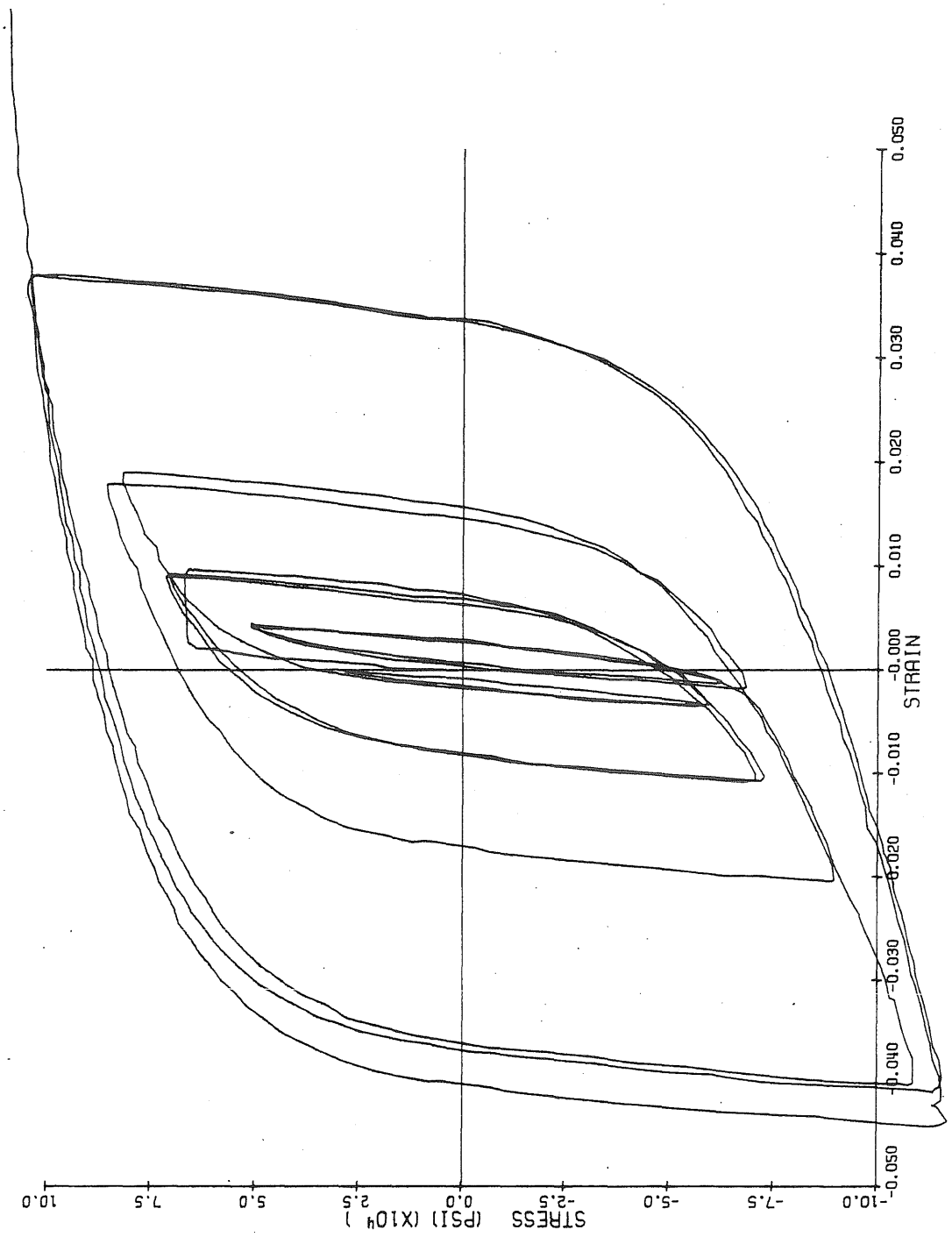

Fig. 6 Test 3, #9 Bar Coupon

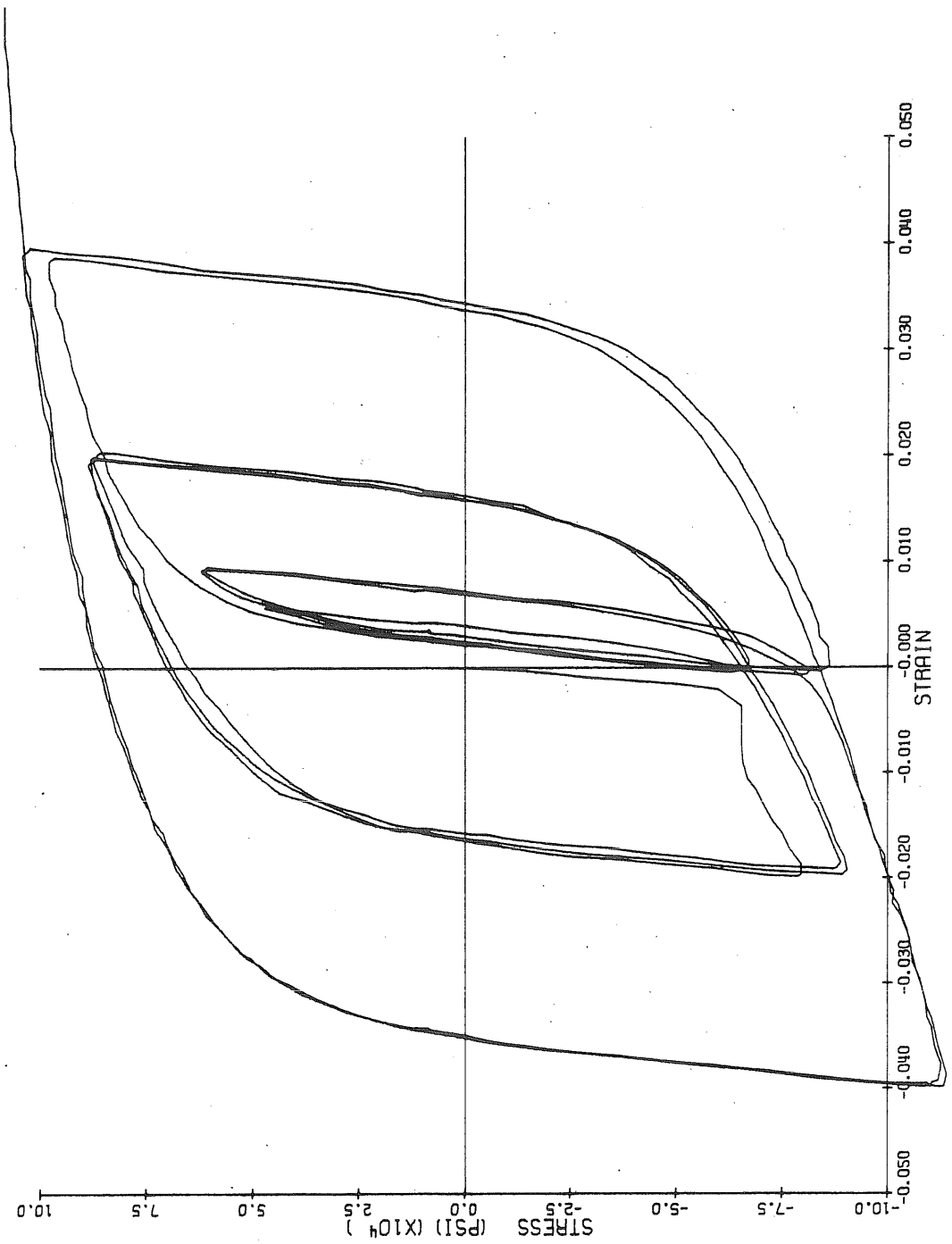

Fig. 7 Test 4, #9 Bar Coupon

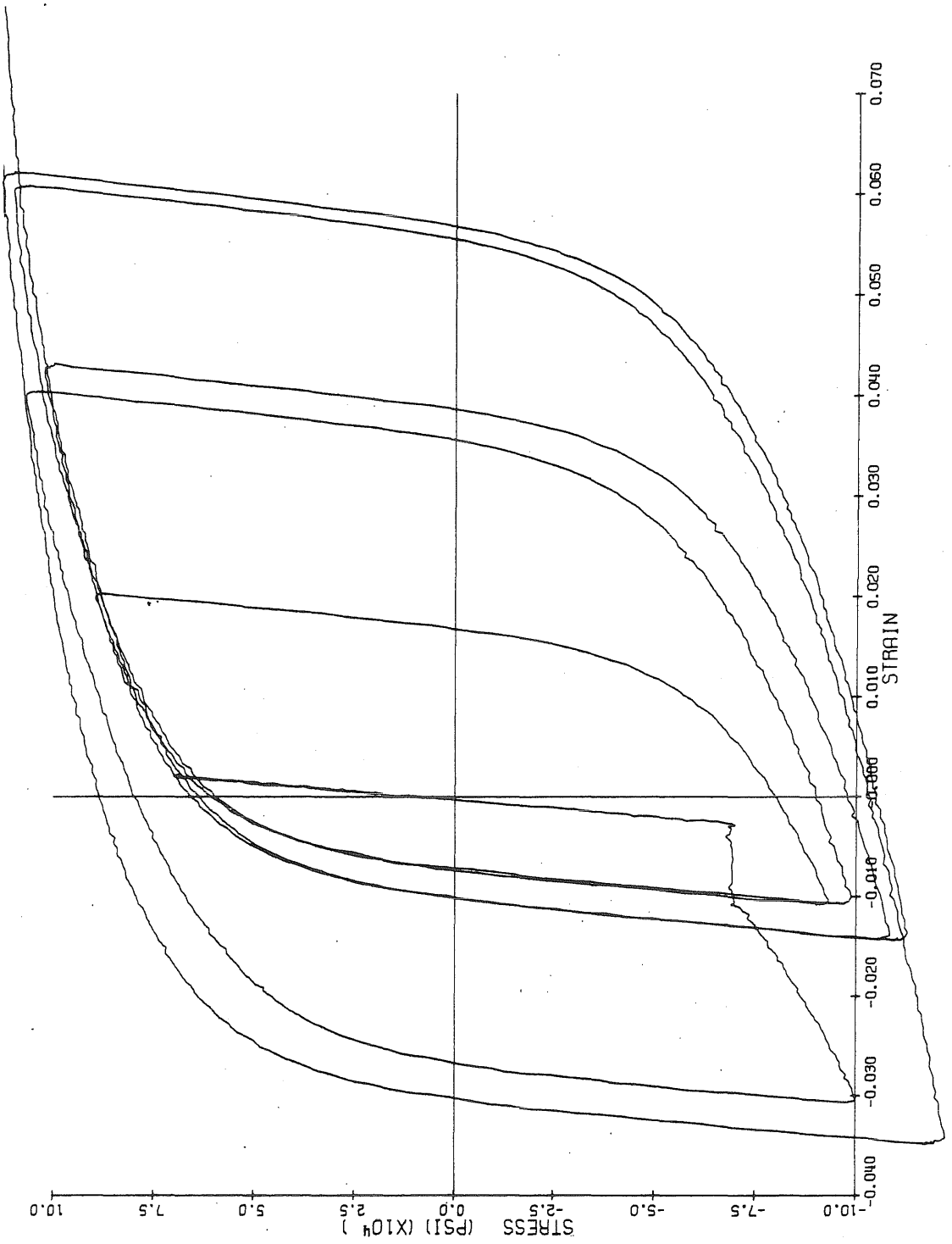

Fig. 8 Test 5, #9 Bar Coupon

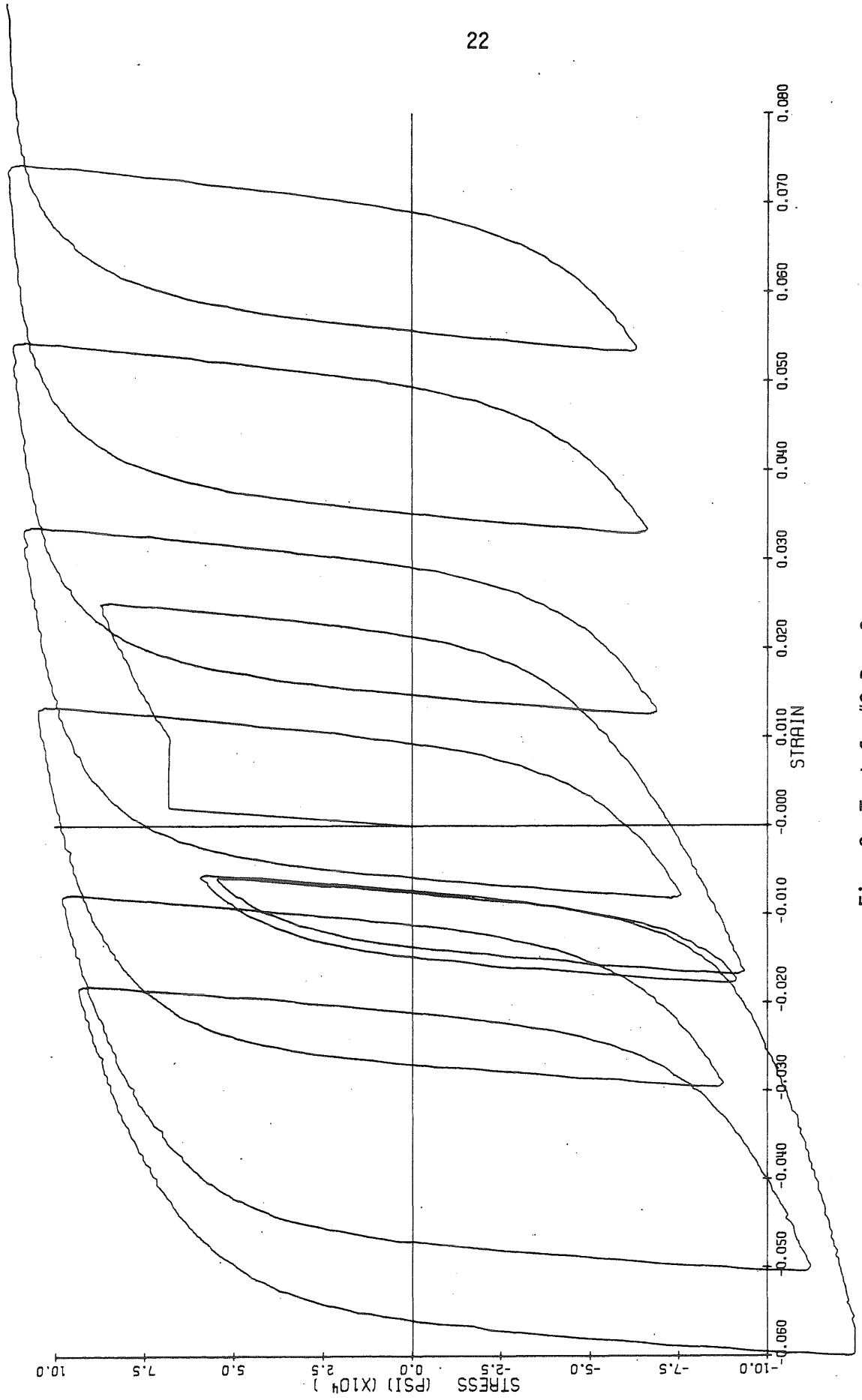

Fig. 9 Test 6, #9 Bar Coupon

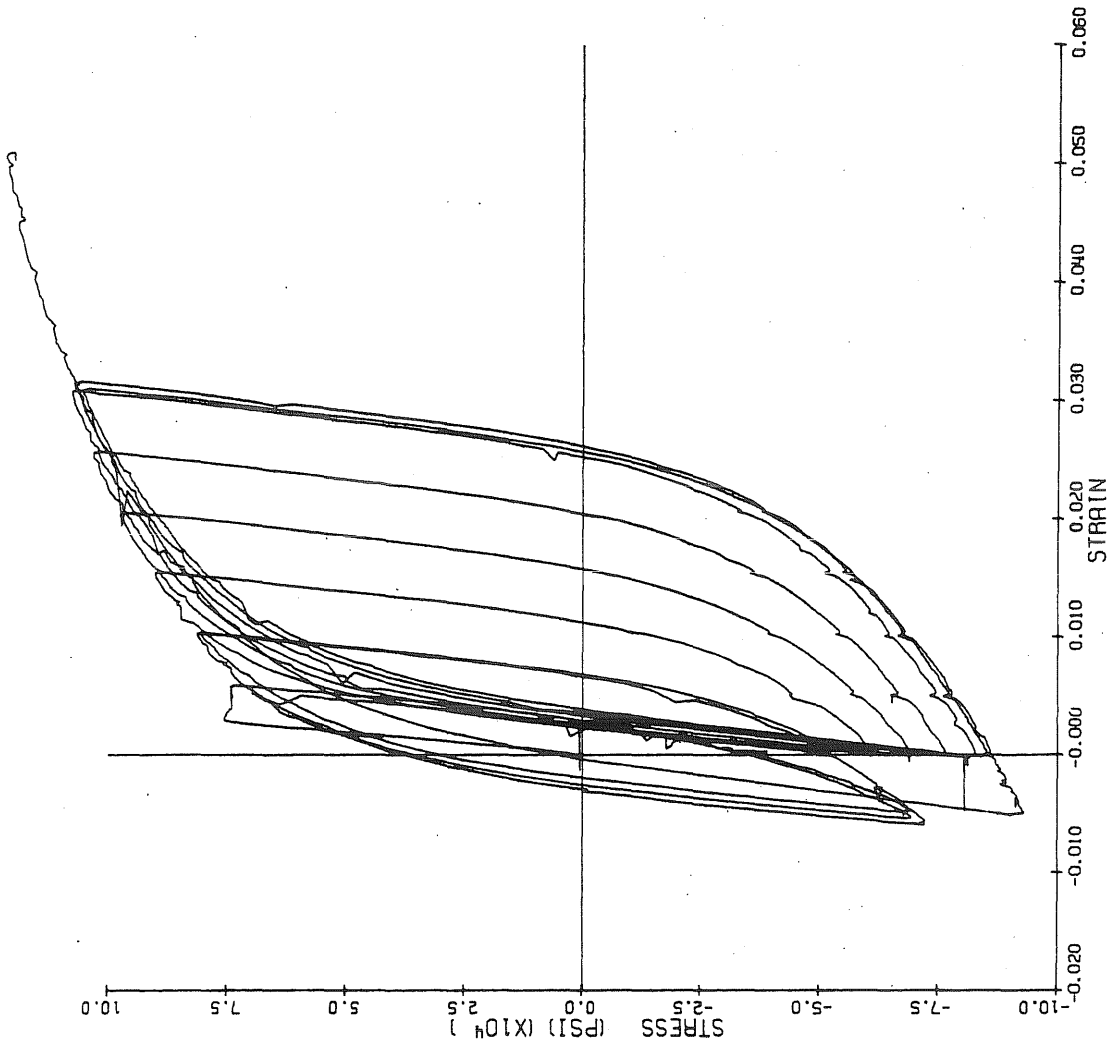

Fig. 10 Test 7, #6 Bar Coupon

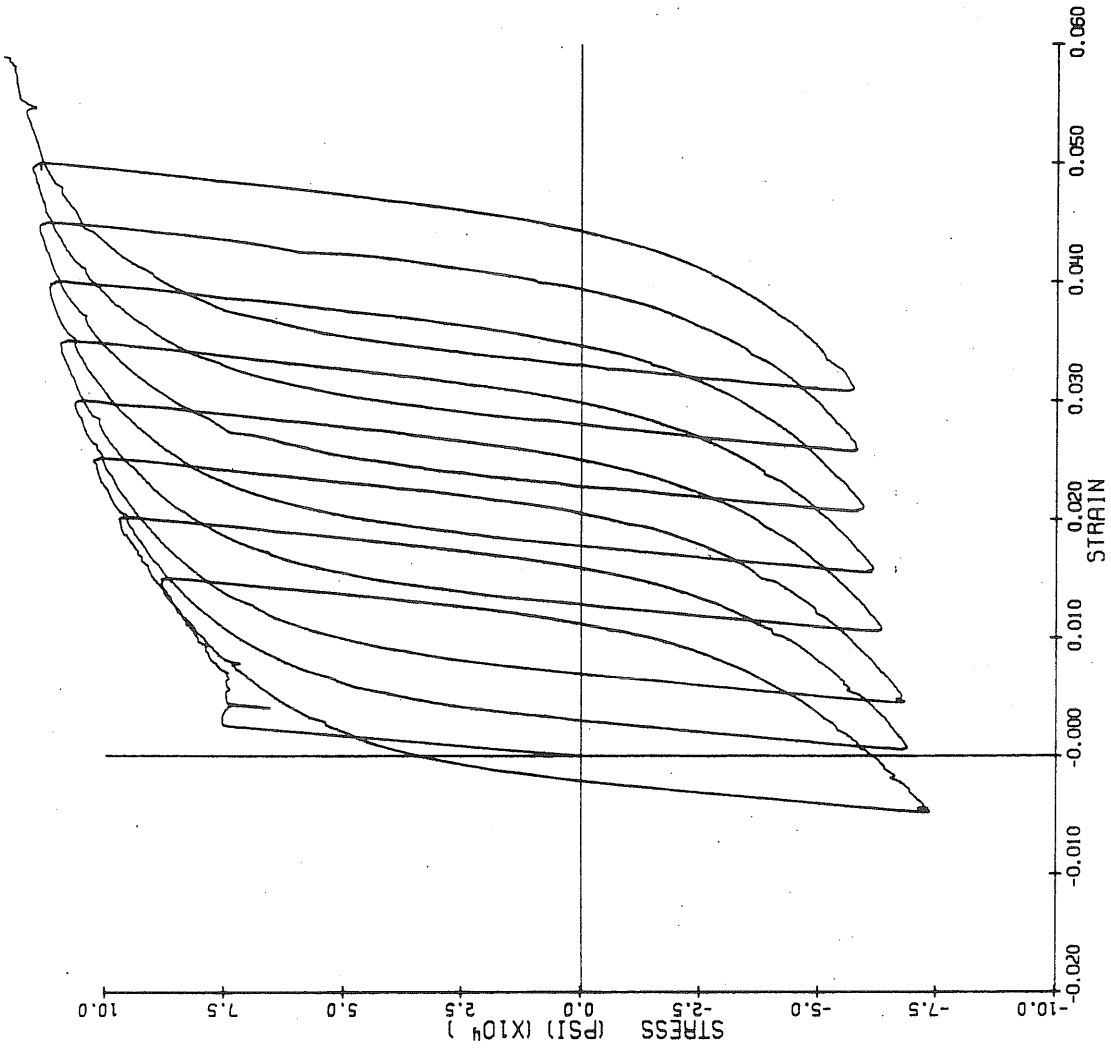

Fig. 11 Test 8, #6 Bar Coupon

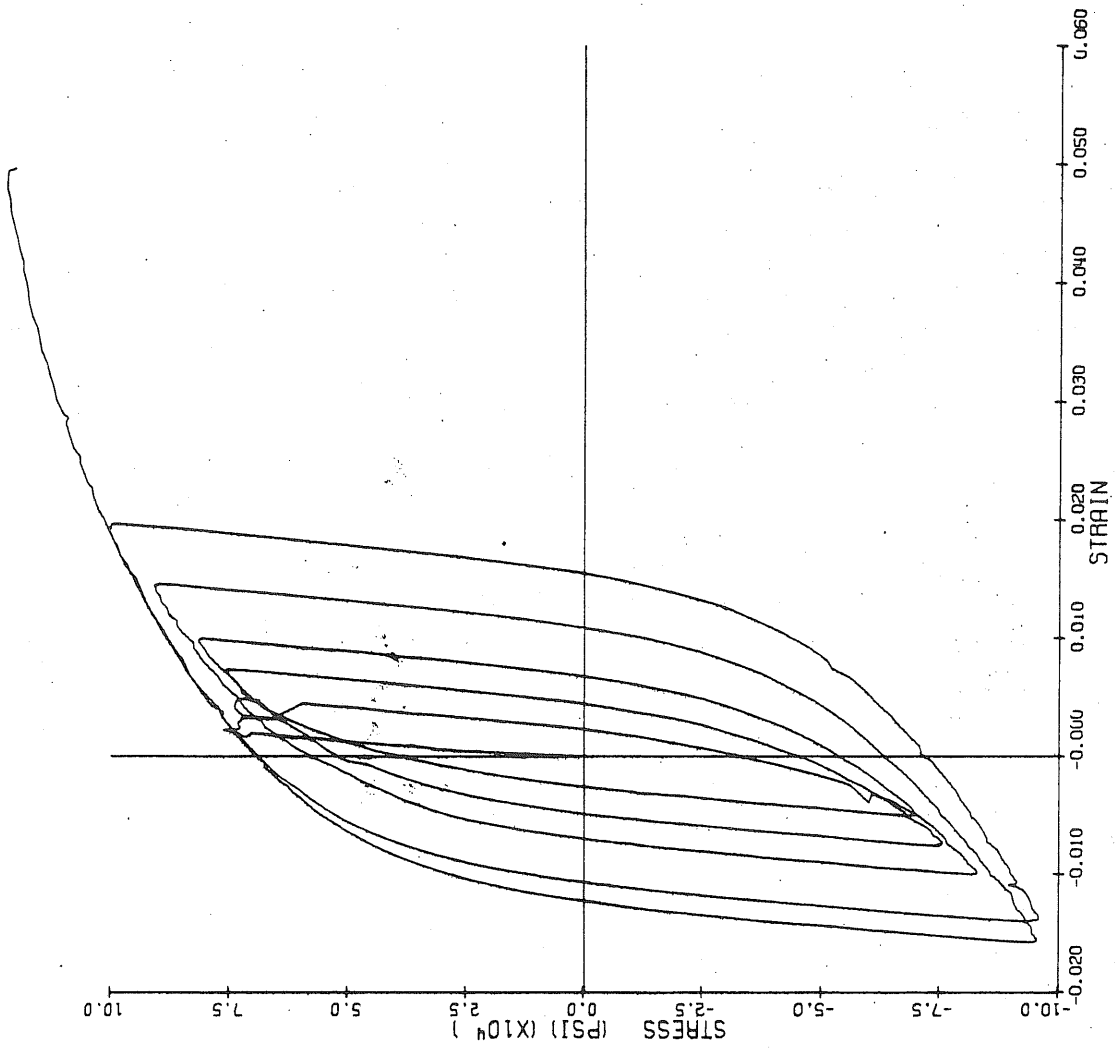

Fig. 12 Test 9, #6 Bar Coupon

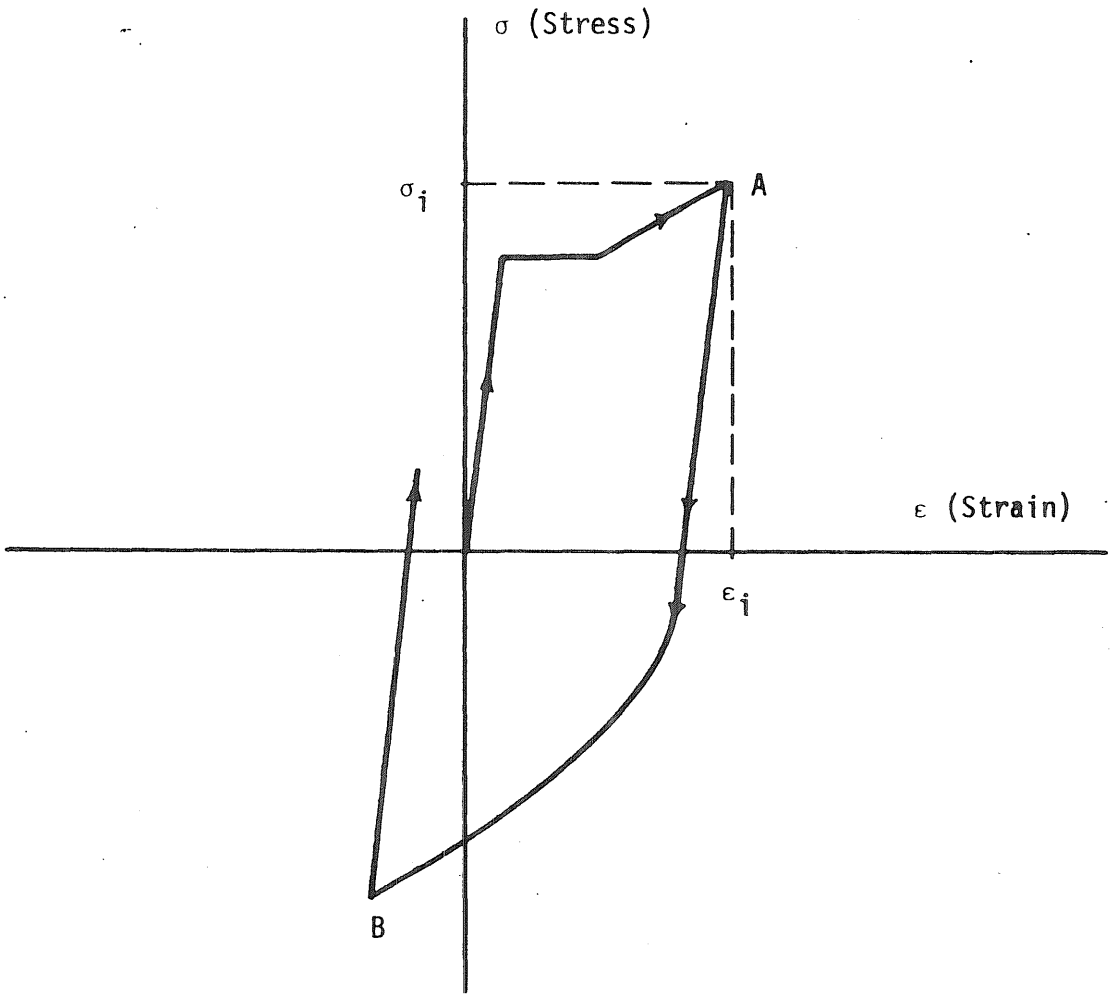

Fig. 13 Initial Stress and Strain for the Half Cycle A-B

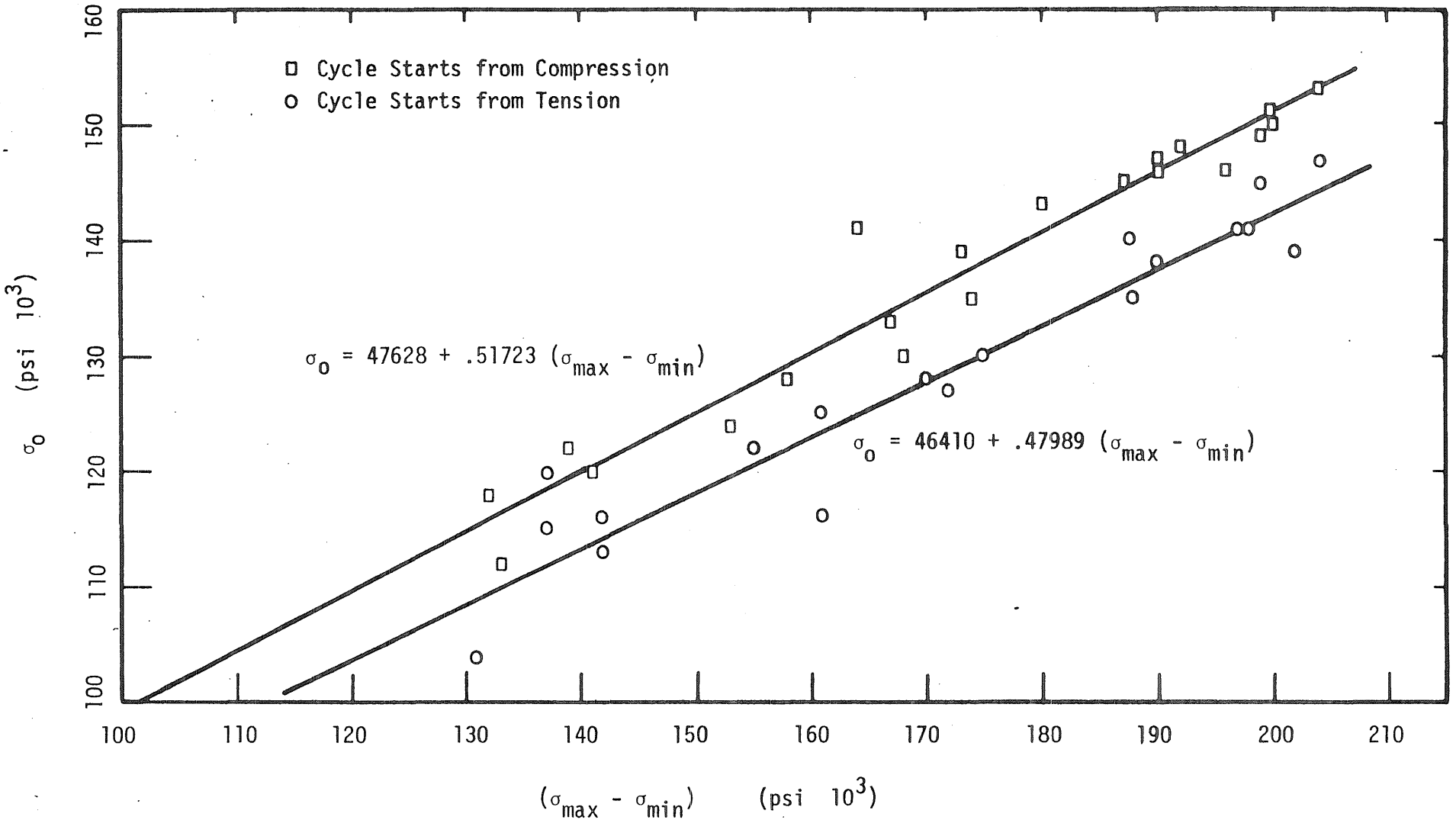

Fig. 14 Plot of σ_o against $(\sigma_{max} - \sigma_{min})$

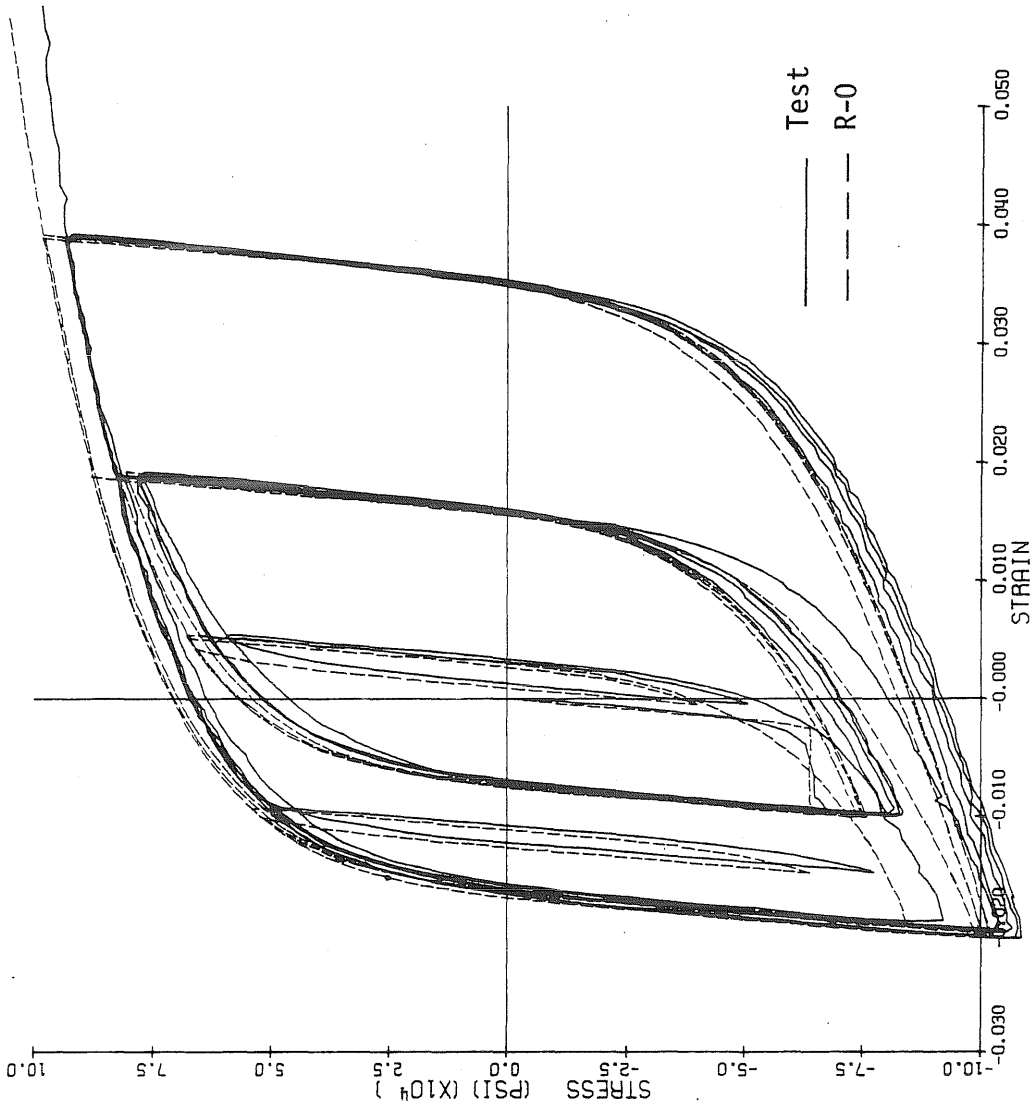

Fig. 15, Test 1, #9 Bar Coupon, Comparison with R-O Model

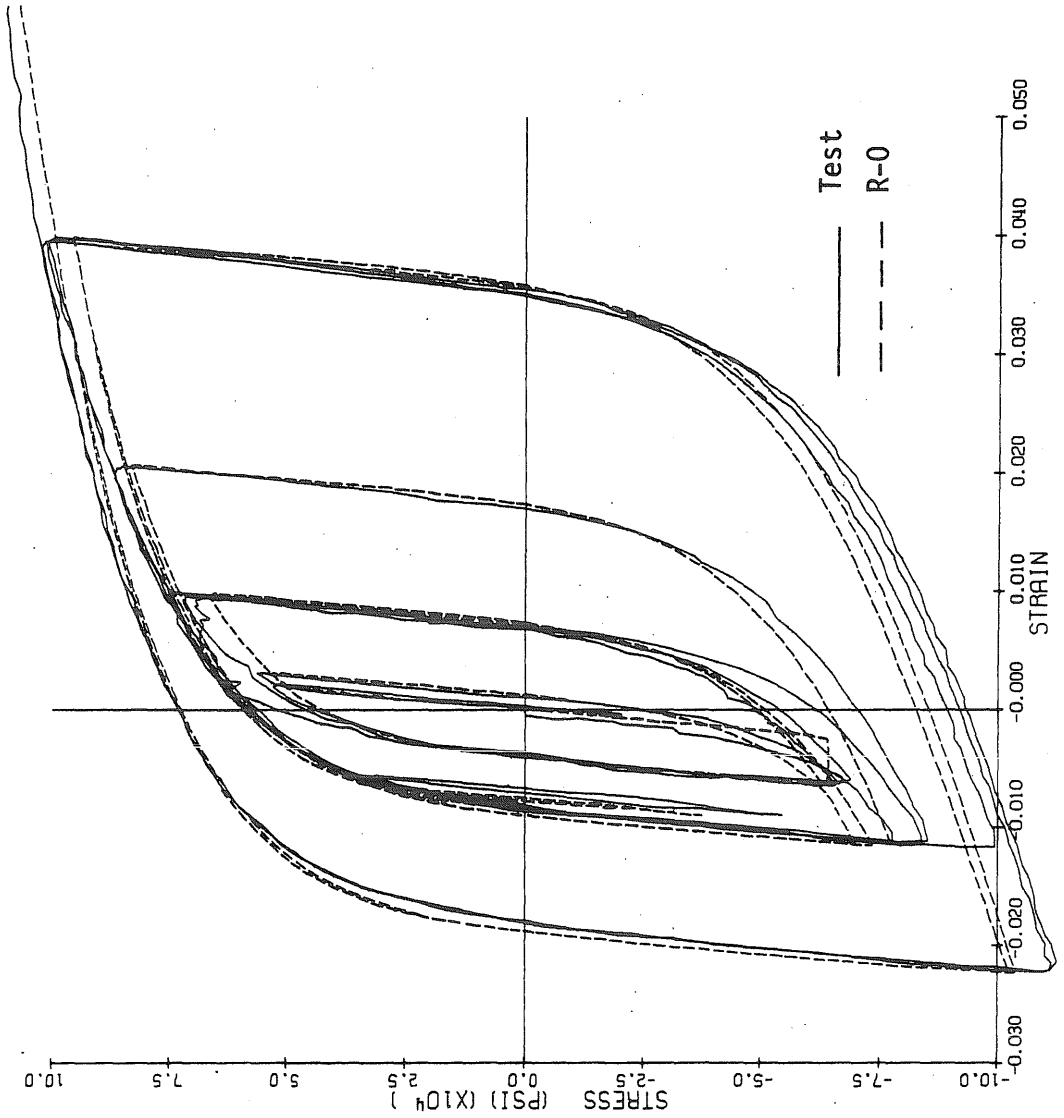

Fig. 16 Test 2, #9 Bar Coupon, Comparison with R-O Model

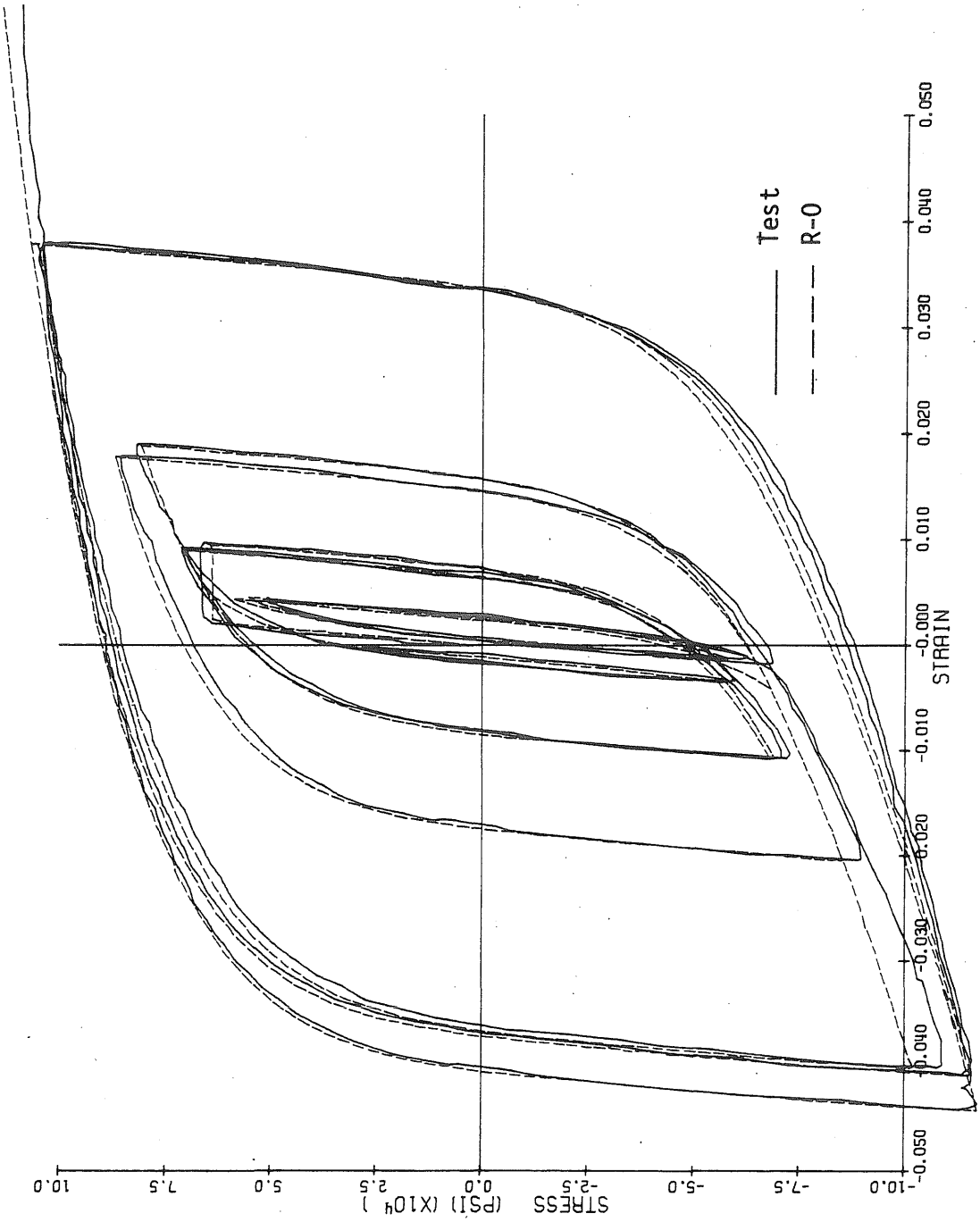

Fig. 17 Test 3, #9 Bar Coupon, Comparison with R-O Model

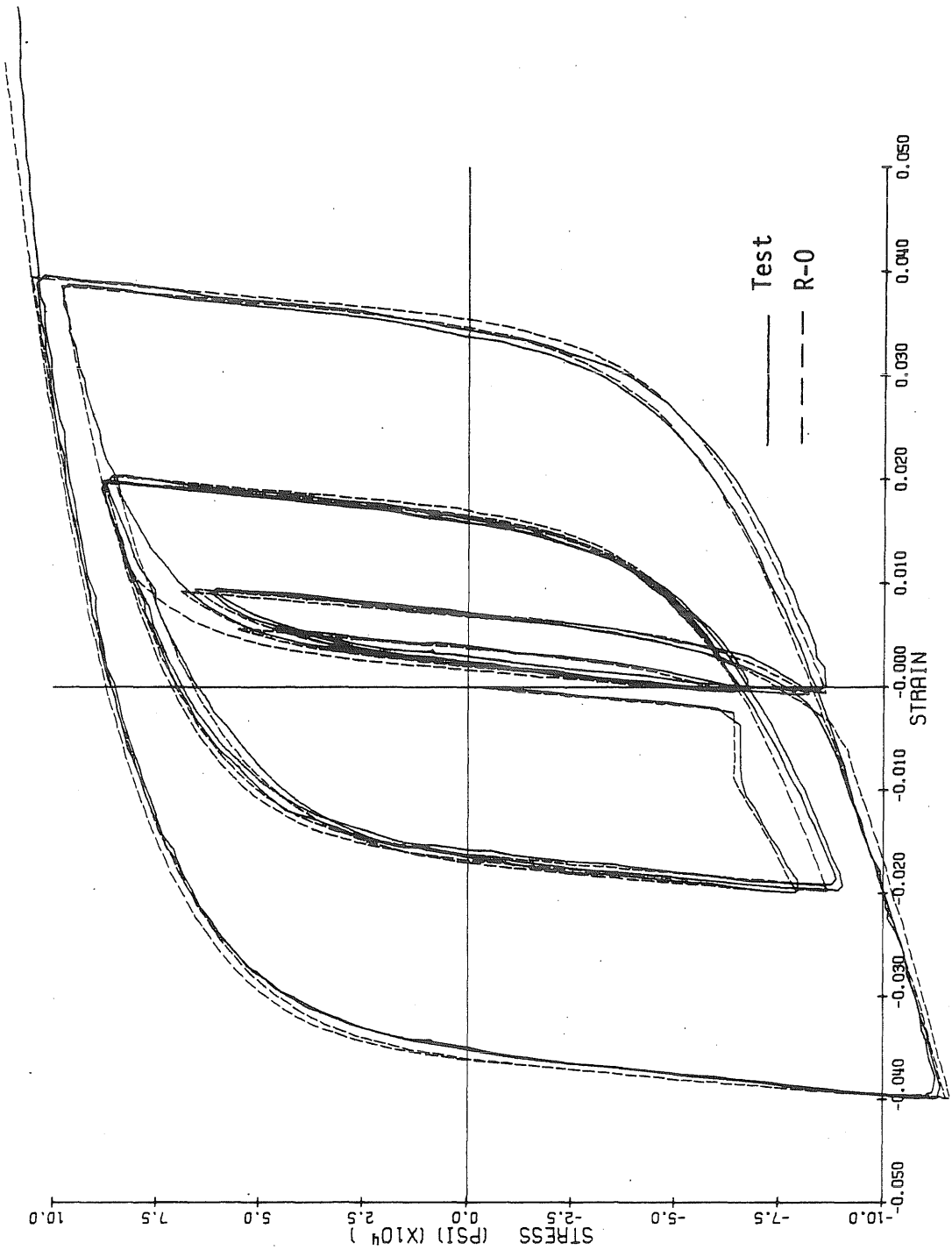

Fig. 18 Test 4, #9 Bar Coupon, Comparison with R-O Model

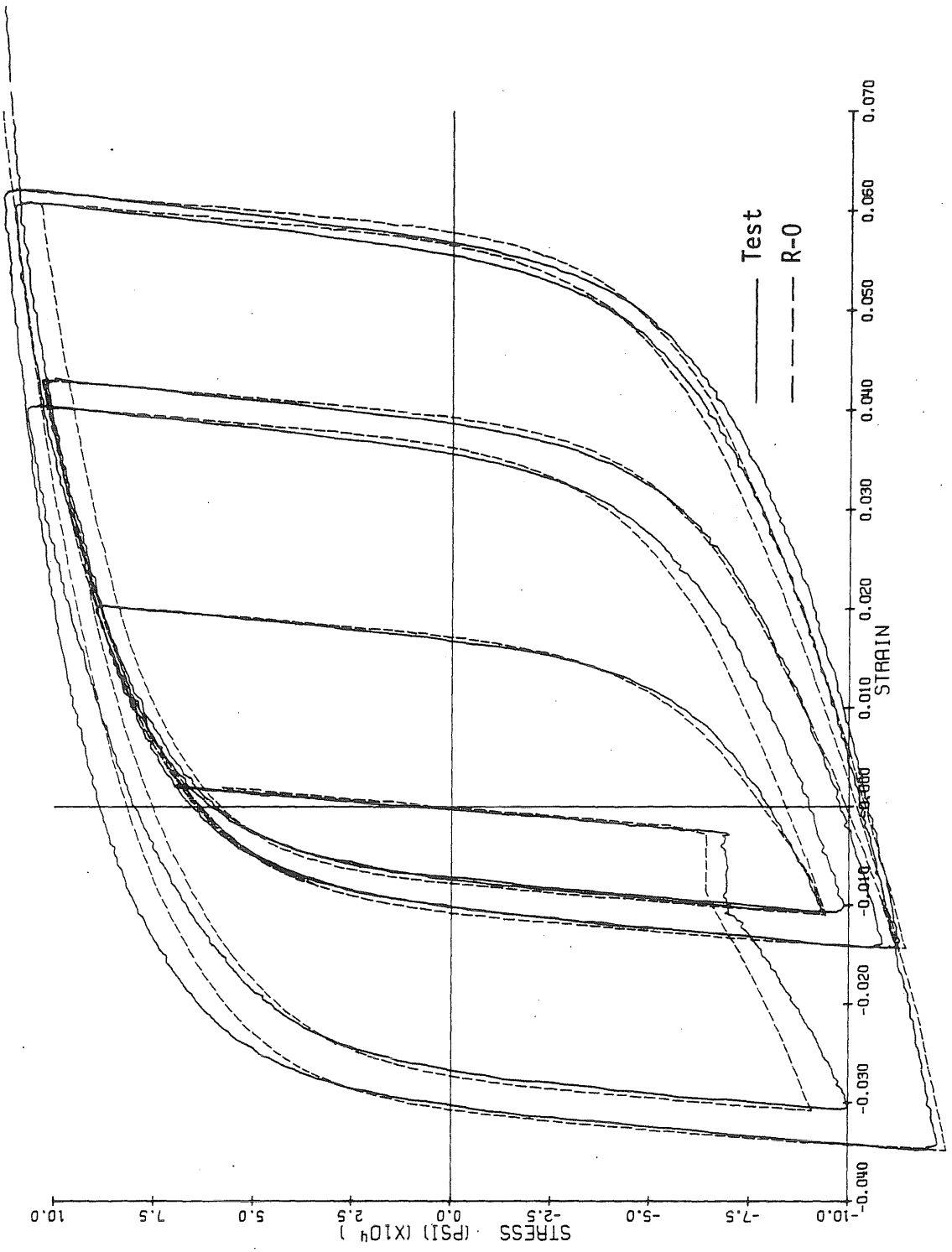

Fig. 19 Test 5, #9 Bar Coupon, Comparison with R-O Model

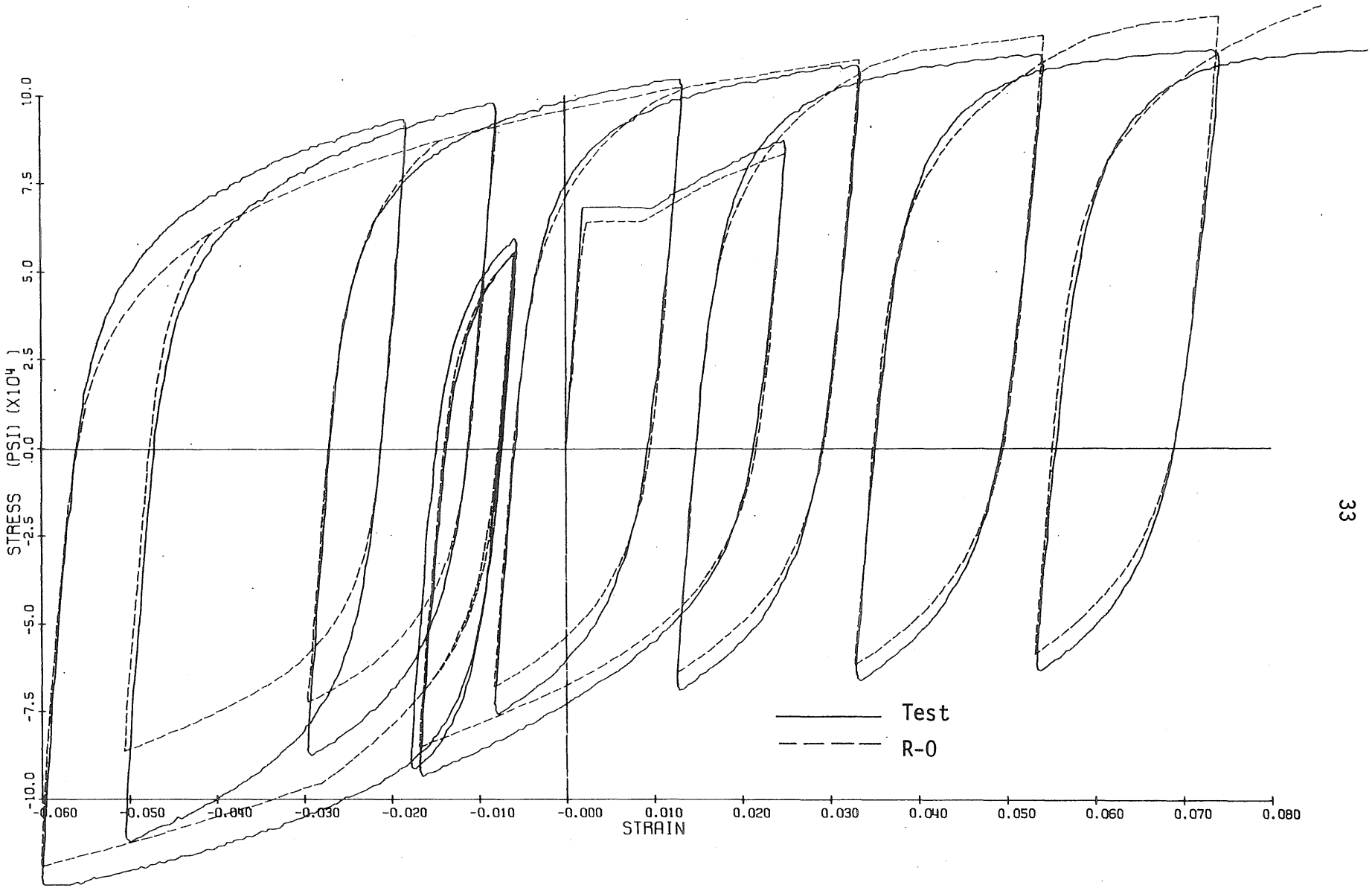

Fig. 20 Test 6, #9 Bar Coupon, Comparison with R-O Model

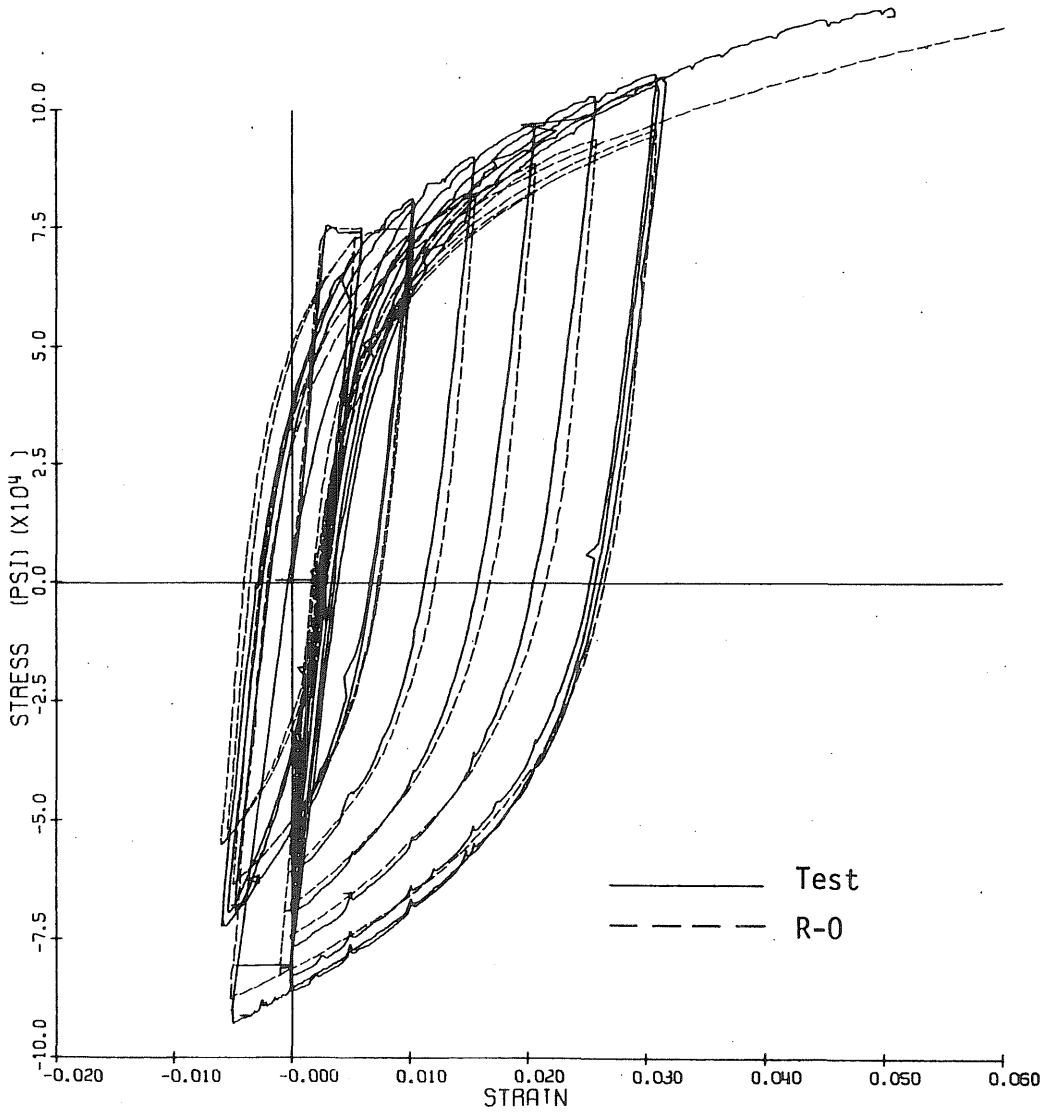

Fig. 21 Test 7, #6 Bar Coupon, Comparison with R-O Model

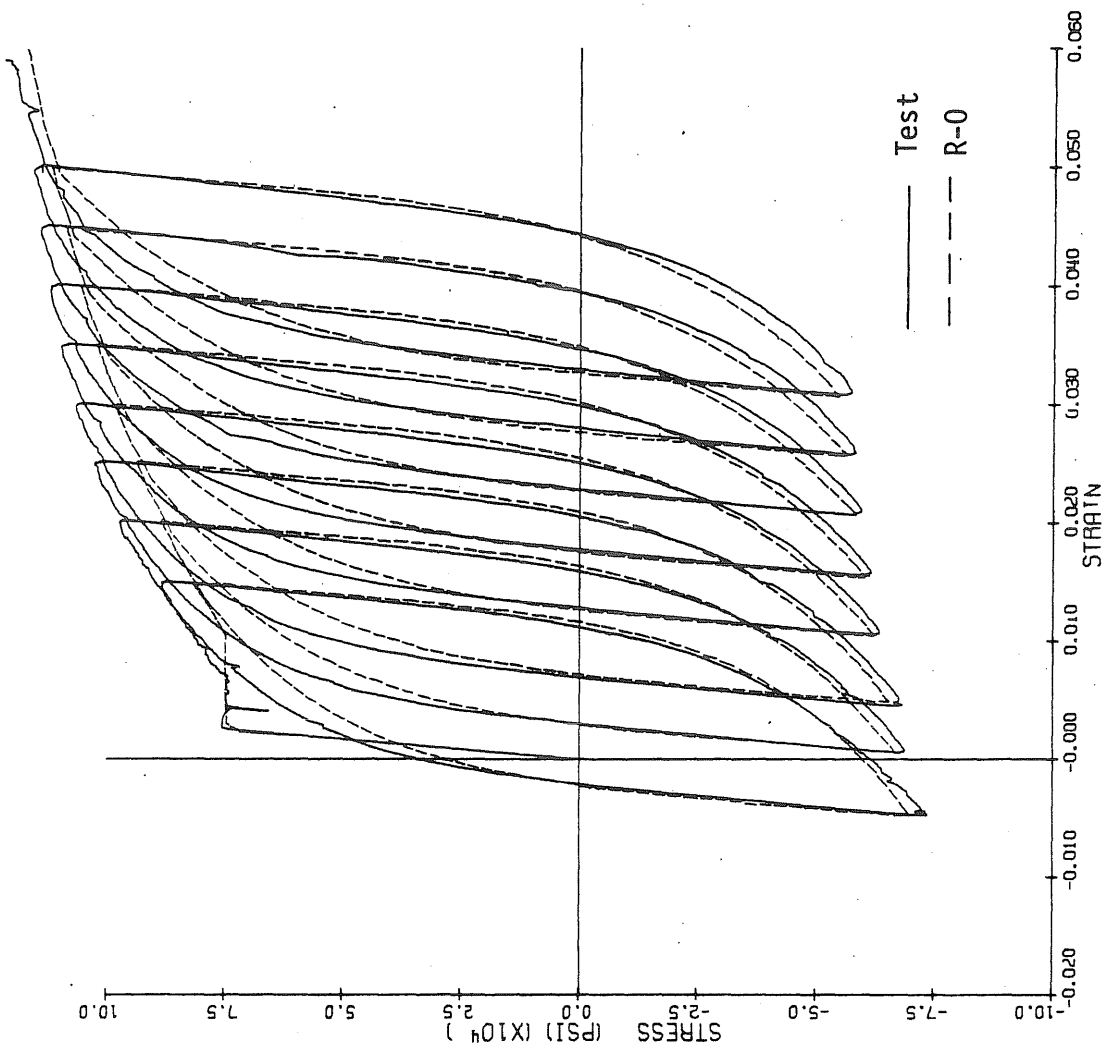

Fig. 22 Test 8, #6 Bar Coupon, Comparison with R-O Model

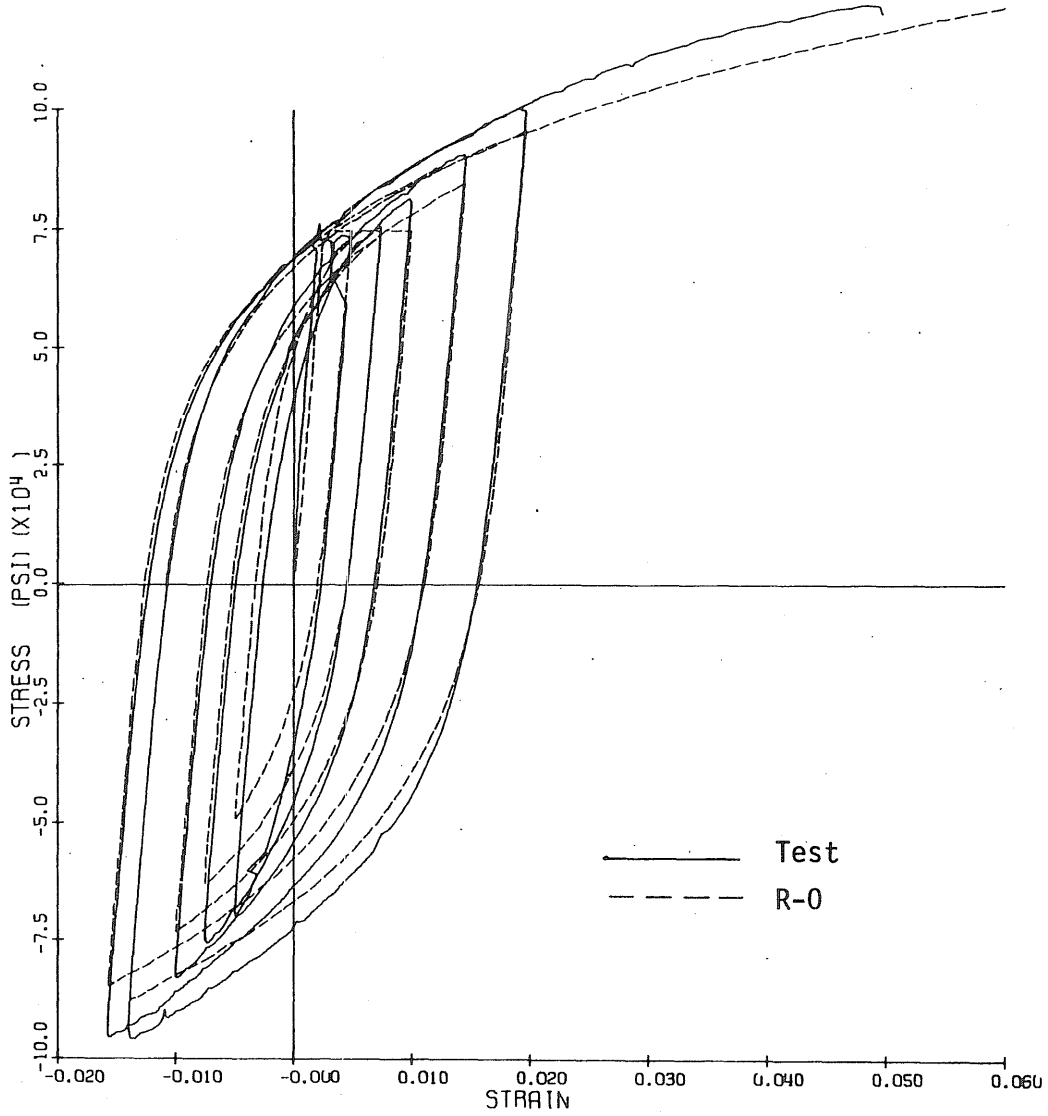

Fig. 23 Test 9, #6 Bar Coupon, Comparison with R-O Model

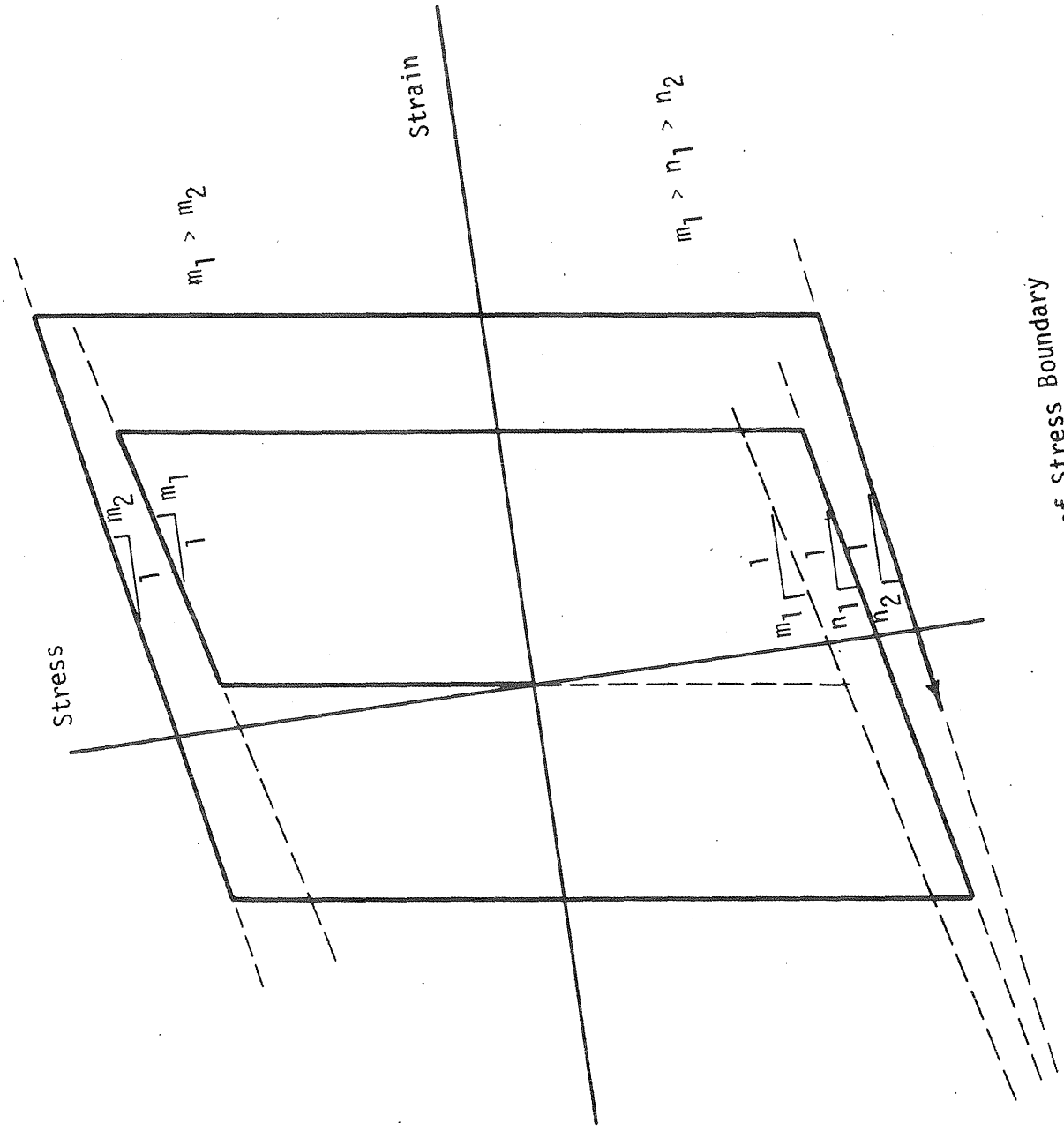

Fig. 24 Change of Stress Boundary

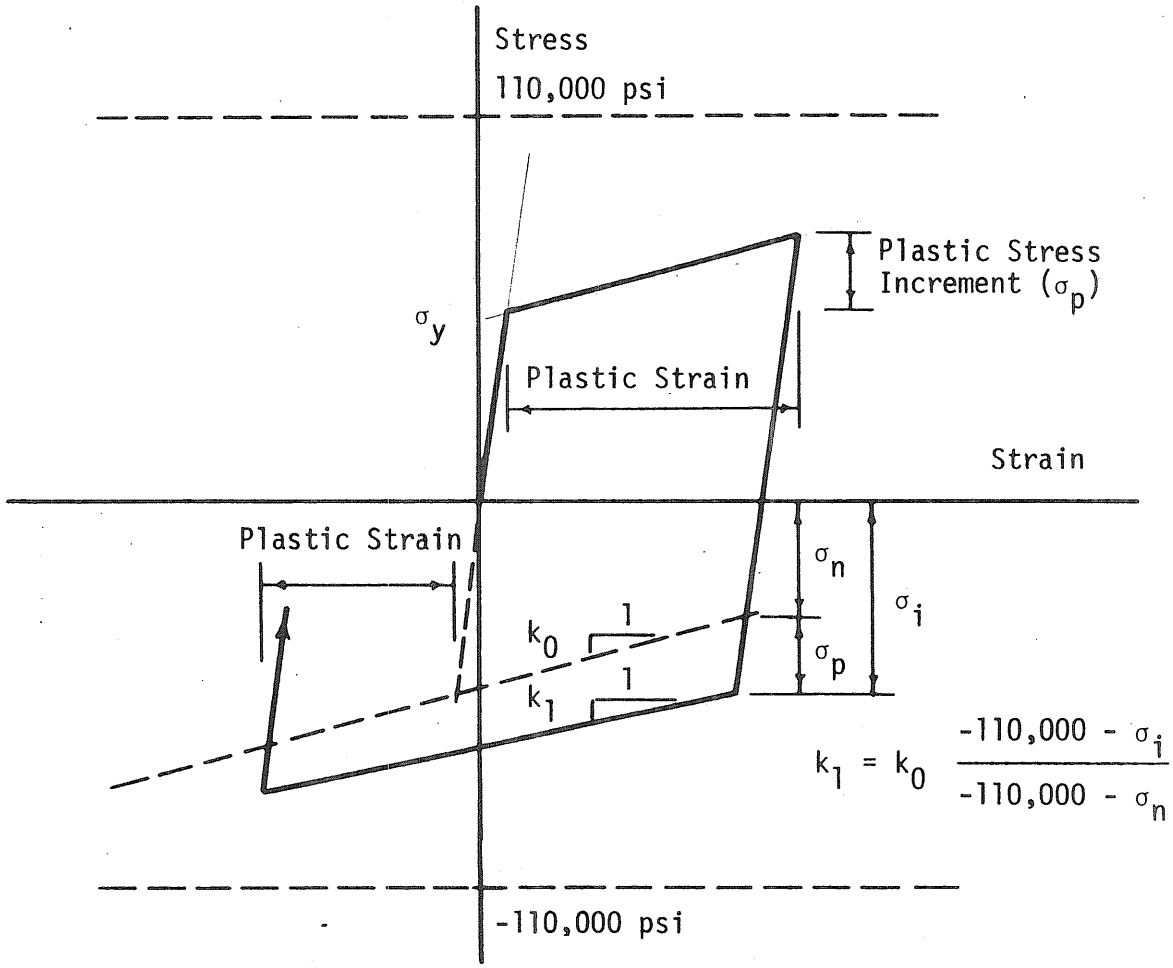

Fig. 25 Linear Stress-Strain Model

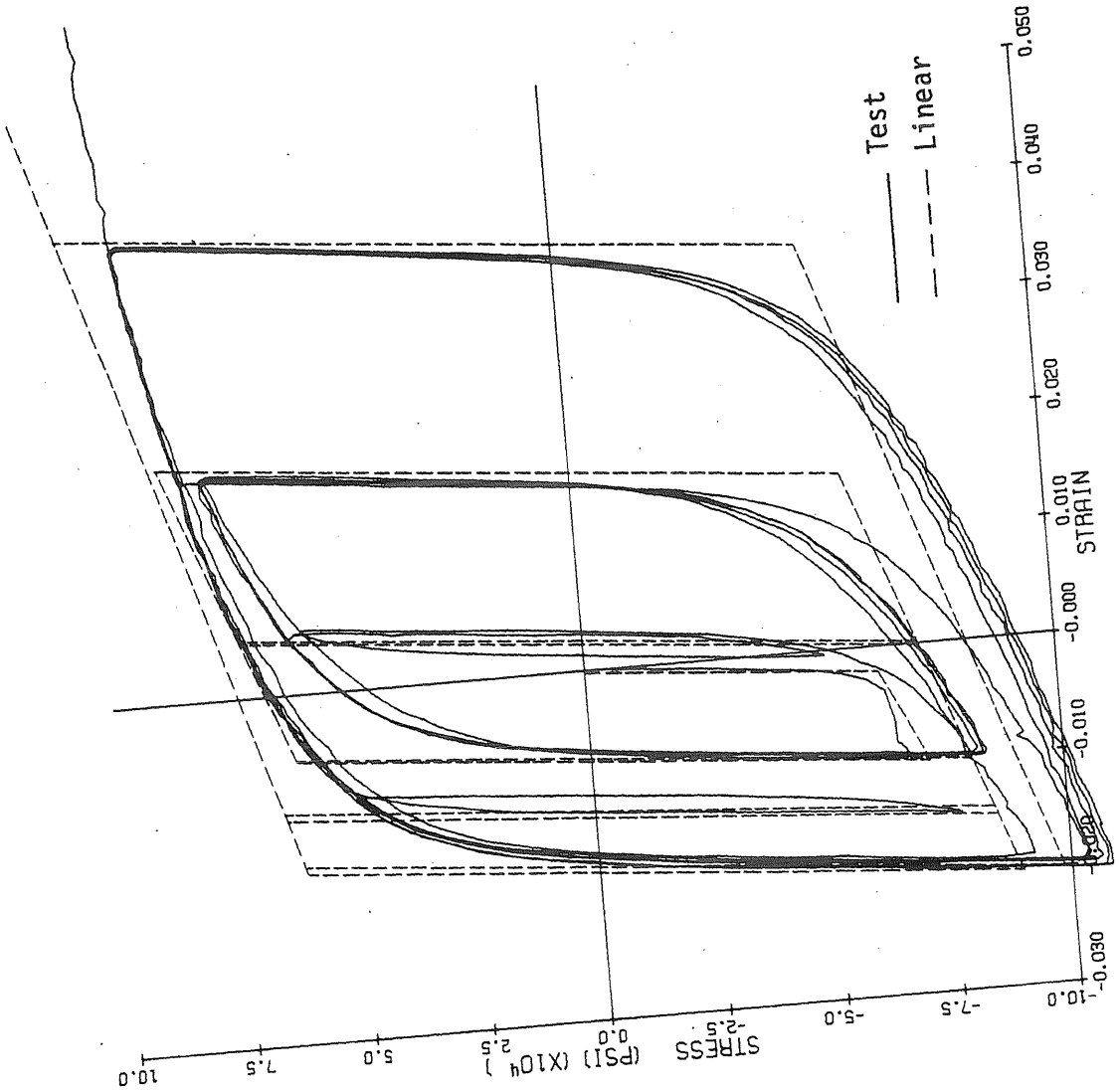

Fig. 26 Test 1, #9 Bar Coupon, Comparison with Linear Model

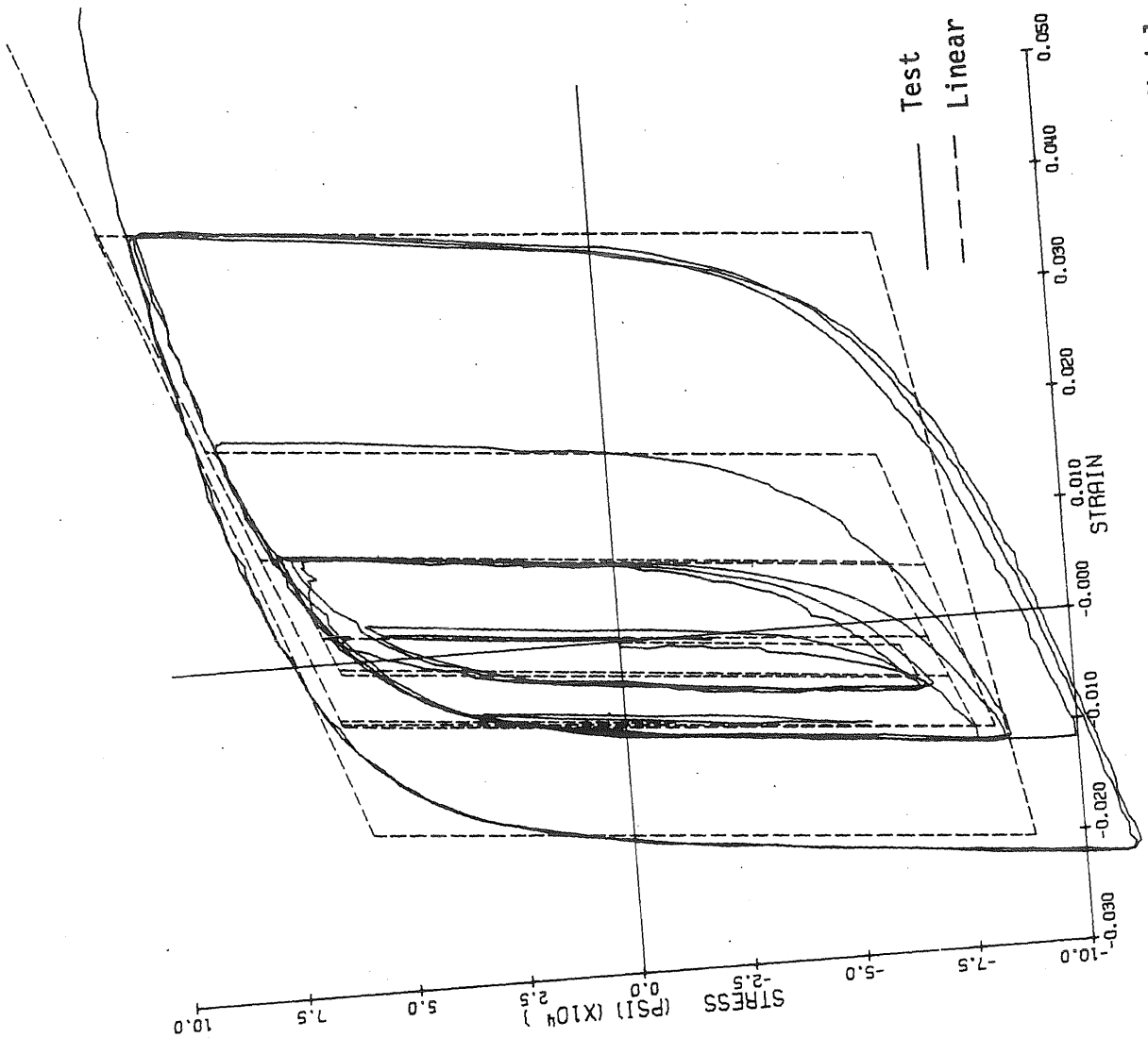

Fig. 27 Test 2, #9 Bar Coupon, Comparison with Linear Model

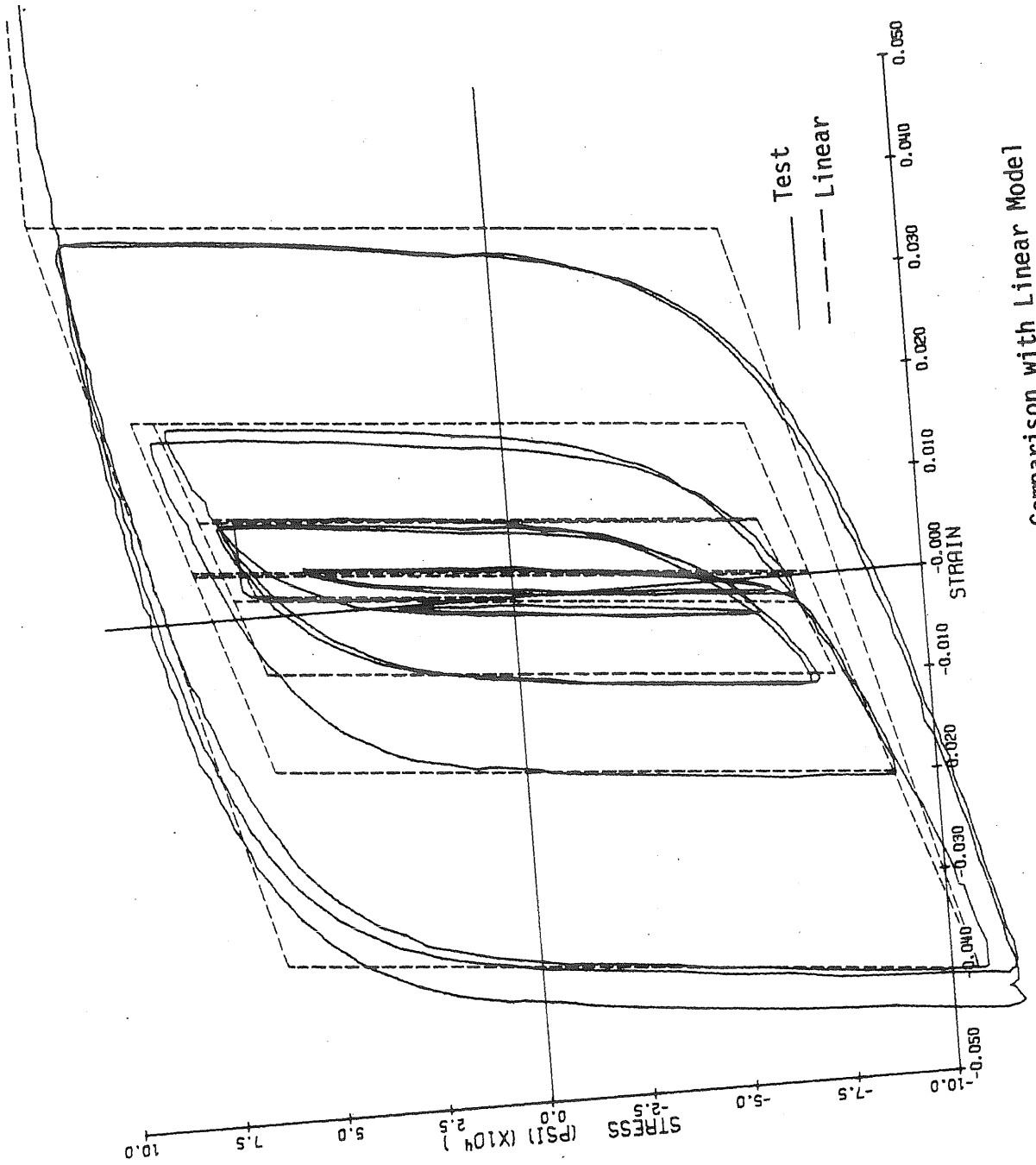

Fig. 28 Test 3, #9 Bar Coupon, Comparison with Linear Model

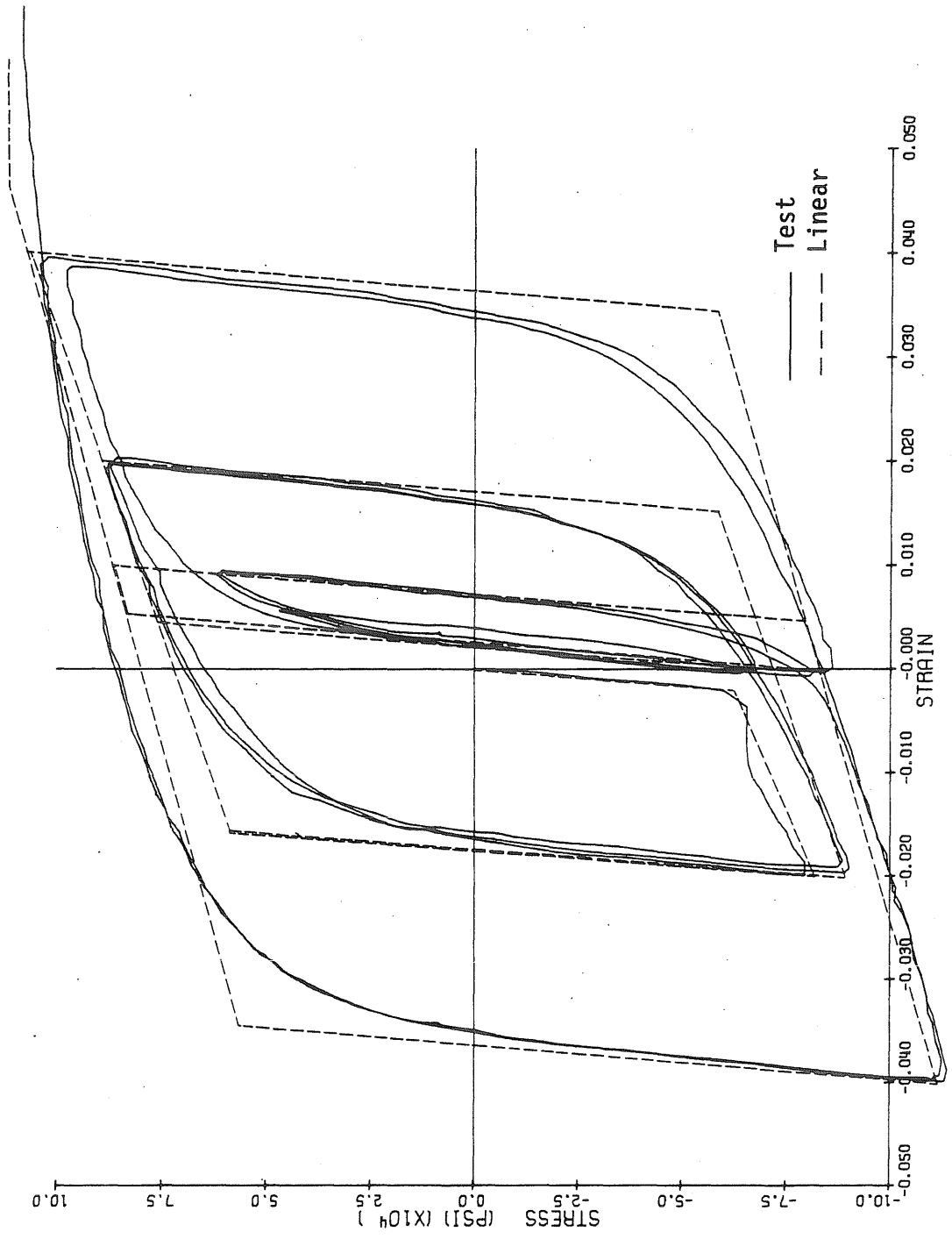

Fig. 29 Test 4, #9 Bar Coupon, Comparison with Linear Model

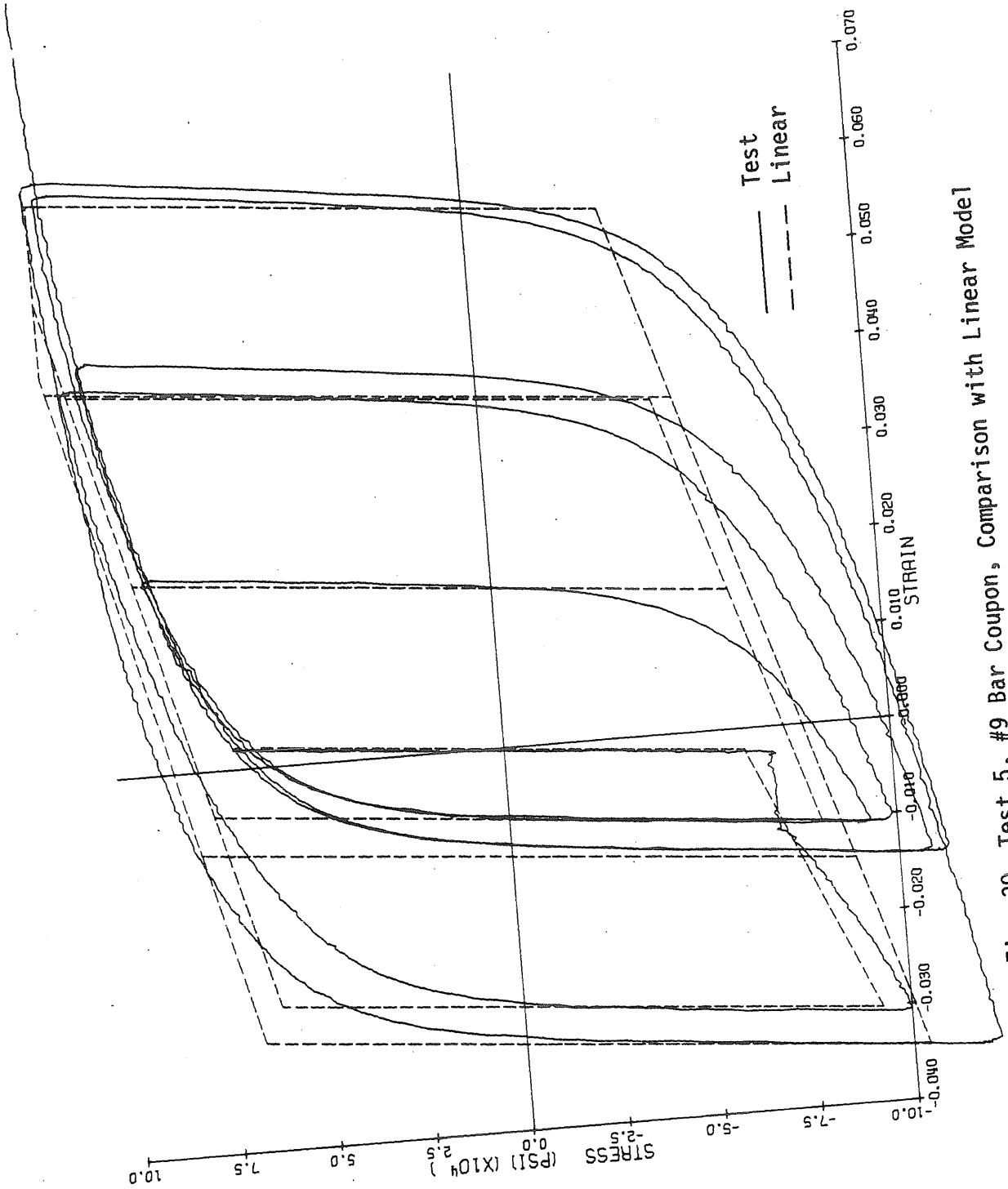

Fig. 30 Test 5, #9 Bar Coupon, Comparison with Linear Model

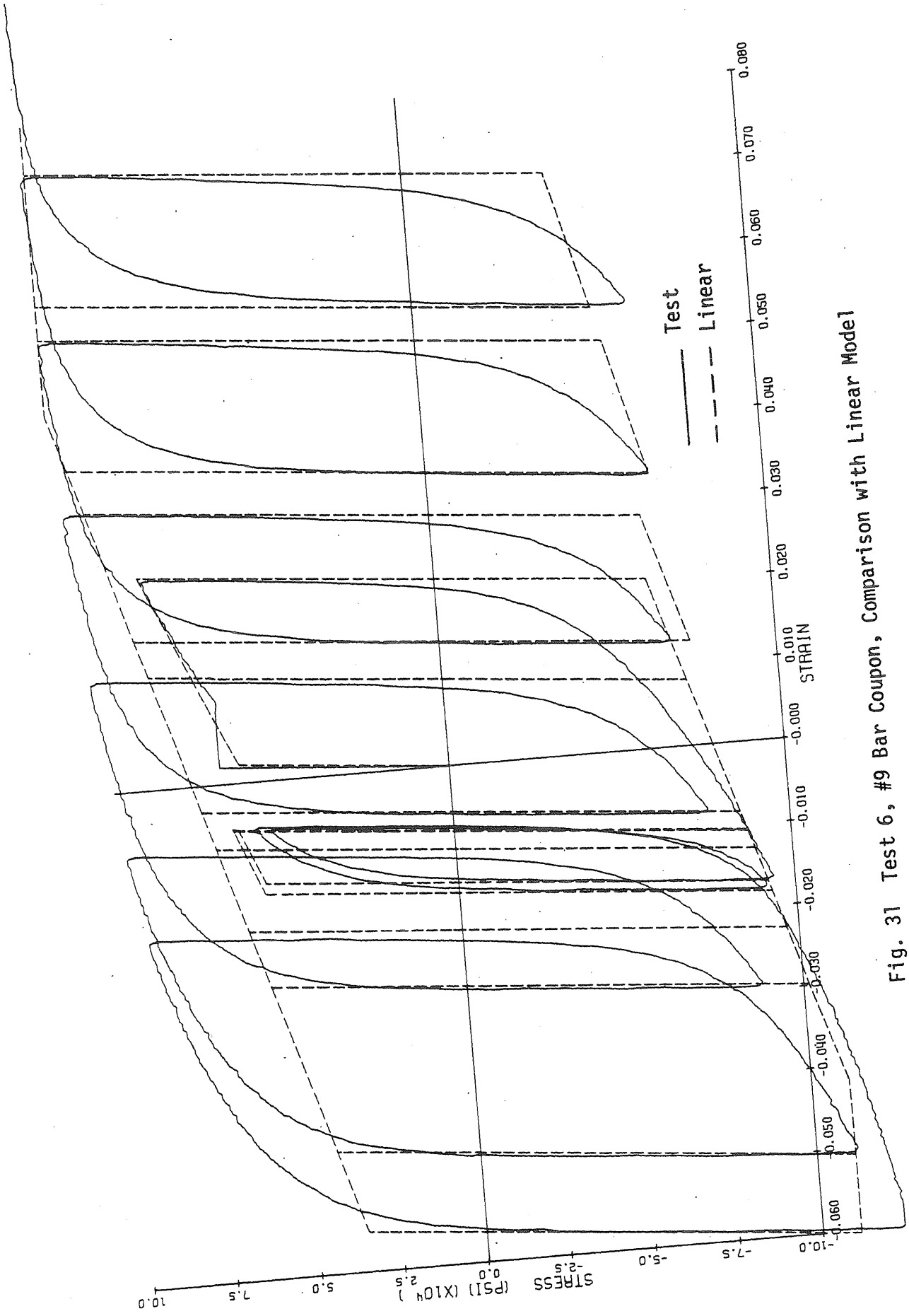

Fig. 31 Test 6, #9 Bar Coupon, Comparison with Linear Model

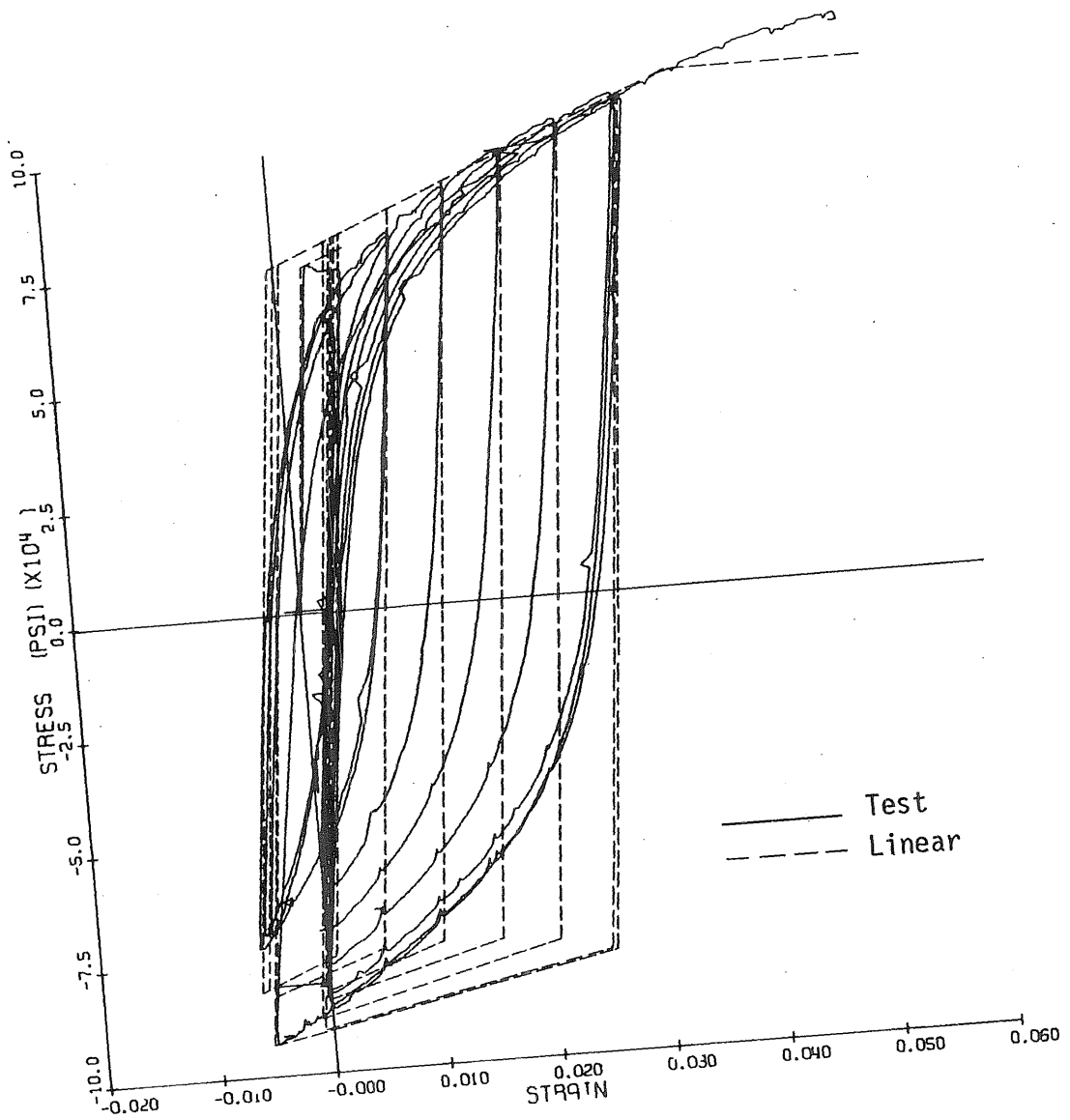

Fig. 32 Test 7, #6 Bar Coupon, Comparison with Linear Model

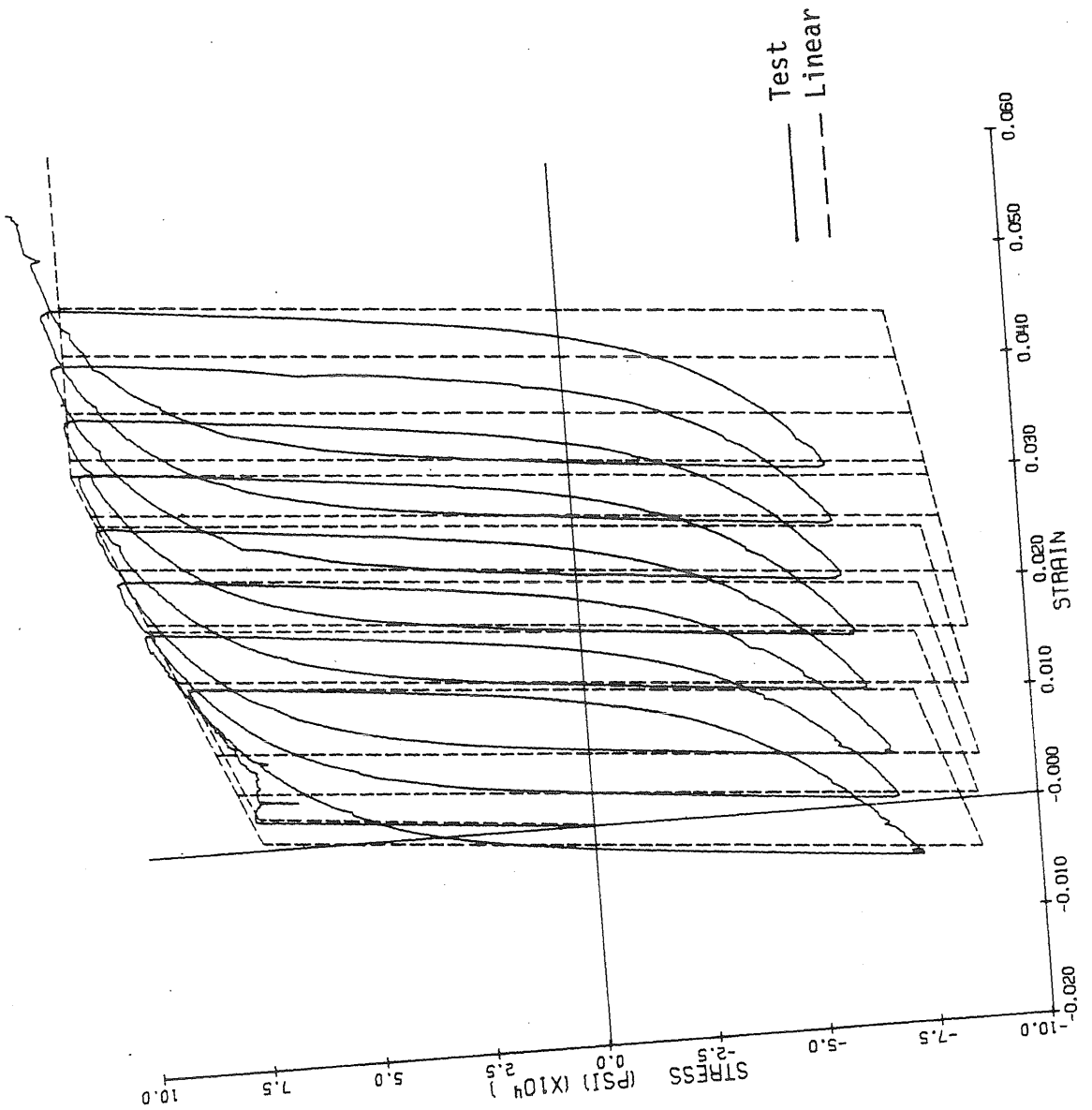

Fig. 33 Test 8, #6 Bar Coupon, Comparison with Linear Model

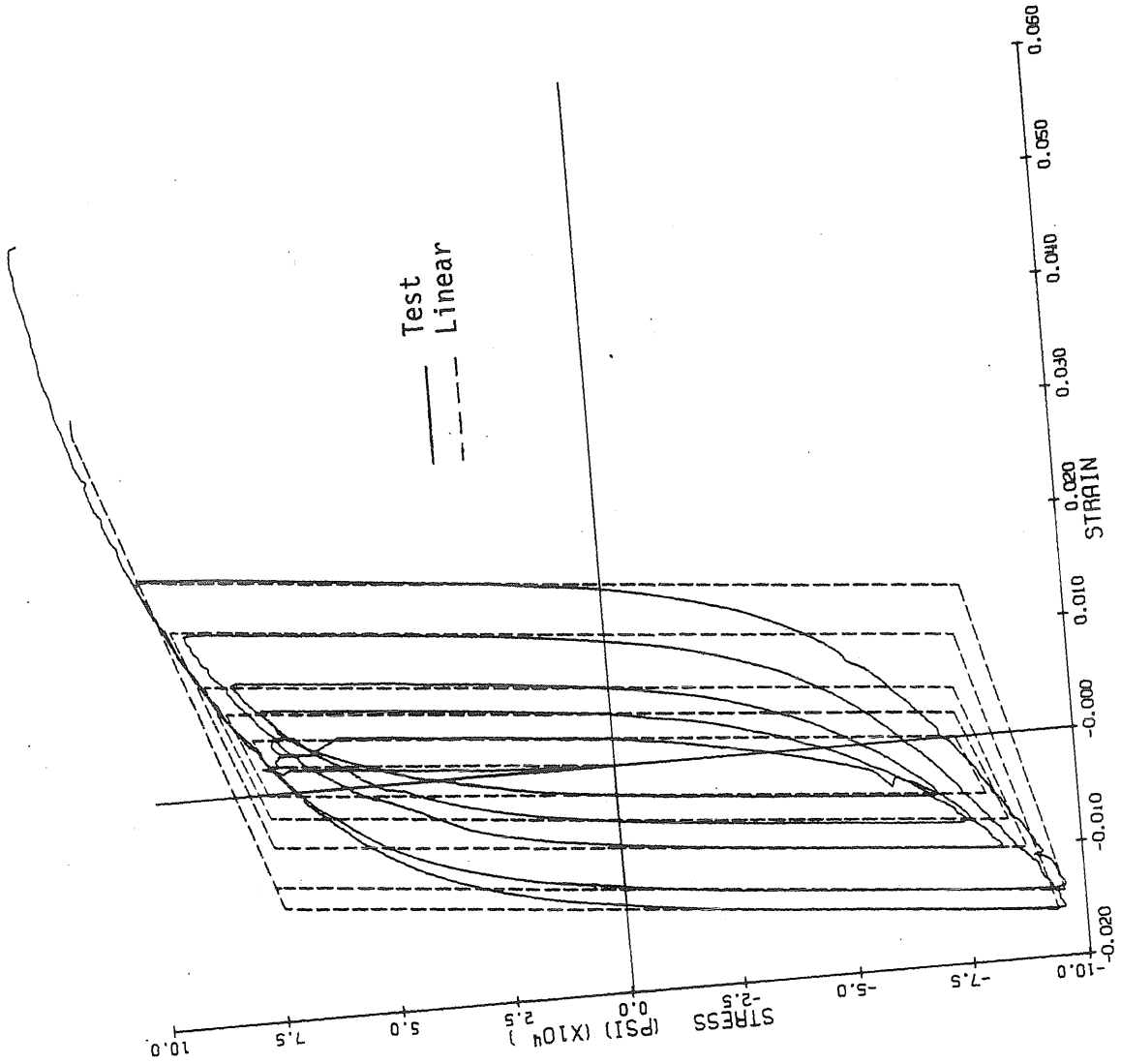

Fig. 34 Test 9, #6 Bar Coupon, Comparison with Linear Model